Trans-encapsidation of hepatitis C virus subgenomic replicon RNA with viral structure proteins

Koji Ishii *, Kyoko Murakami, Su Su Hmwe, Bin Zhang, Jin Li, Masayuki Shirakura, Kenichi Morikawa, Ryosuke Suzuki, Tatsuo Miyamura, Takaji Wakita, Tetsuro Suzuki

Department of Virology II, National Institute of Infectious Diseases, 1-23-1 Toyama, Shinjuku-ku, Tokyo 162-8640, Japan

ARTICLE INFO

ABSTRACT

A trans-packaging system for hepatitis C virus (HCV) subgenomic replicon RNAs was developed. HCV subgenomic replicon was efficiently encapsidated by the HCV structural proteins that were stably expressed *in trans* under the control of a mammalian promoter. Infectious HCV-like particles (HCV-LPs), established a single-round infection, were produced and released into culture medium in titers of up to 10^3 focus forming units/ml. Expression of NS2 protein with structural proteins (core, E1, E2, and p7) was shown to be critical for the infectivity of HCV-LPs. Anti-CD81 treatment decreased the number of infected cells, suggesting that HCV-LPs infected cells in a CD81-dependent manner. The packaging cell line should be useful both for the production of single-round infectious HCV-LPs to elucidate the mechanisms of HCV assembly, particle formation and infection to host cells, and for the development of HCV replicon-based vaccines.

© 2008 Elsevier Inc. All rights reserved.

Hepatitis C virus (HCV) is a positive-strand RNA virus that belongs to the *Hepacivirus* genus in the *Flaviviridae* family. The HCV genome comprises about 9600 nucleotides that encode a single polyprotein of around 3000 amino acids [1–3], which is processed by cellular and viral encoded proteases into at least 10 different structural and nonstructural proteins [4–6]. The JFH-1 strain of HCV, classified as genotype 2a strain, is the first HCV strain that can produce HCV particles in Huh7 cells [7,8]. The synthesis of HCV-like particles (HCV-LPs) using a recombinant baculovirus containing the cDNA of HCV structural proteins has been reported [9]. HCV-LP production by mammalian expression systems using vesicular stomatitis virus [10] and semliki forest virus [11] were also reported although the amount of VLP production is not as high as that of baculovirus system.

Subgenomic replicon system is a useful tool as gene expression vectors and is desirable for the development of vaccines. In the case of flaviviruses, several systems have been described for packaging flavivirus replicons, including Kunjin virus replicons [12–14], yellow fever virus replicons [15], tick-borne encephalitis virus replicons [16], and West Nile virus replicons [17,18]. In some cases, these packaging systems have utilized cell lines expressing the flavivirus structural proteins under the control of eukaryotic promoters [16,19]. These virus-like particle (VLP)-generating systems have been useful for packaging viral genomes encoding various foreign genes [14,15,20,18], the study of virus tropism and various aspects of viral assembly and entry [17].

Subgenomic replicons of JFH-1 replicate efficiently in Huh7 cells and do not require cell culture-adaptive mutations [21]. The construction of a system to package HCV replicon into HCV-LPs would not only be useful to investigate as-yet unclear steps of HCV life cycles such as genome packaging and virion assembly but also offers the possibilities of a new approach for vaccine development. In this study, we constructed subgenomic replicon cell lines constitutively expressing JFH-1 structural proteins under the control of elongation factor-1α (EF) promoter, and found stable expression of structural proteins and release of HCV-LPs from the cell line. A sucrose density gradient centrifugation of the culture medium resulted in partial purification of the HCV-LPs. Infectivity of HCV-LPs produced by this system was confirmed by colony formation assay and immunofluorescence analysis. Anti-CD81 antibody treatment decreased the infectivity of HCV-LPs, suggesting that VLPs infected to cells in CD81-dependent fashion. This is the first report that HCV structural proteins of HCV can trans-package its subgenomic replicon. The system described here should be useful to elucidate the mechanisms of HCV assembly, particle formation, and infection to host cells.

Materials and methods

Plasmid construction. Core to p7 coding region of JFH-1 was amplified using pJFH-1 [21] as a template and sense primer

---

* Corresponding author. Fax: +81 3 5285 1161.
E-mail address: kishii@nih.go.jp (K. Ishii).

5'-GAGAATTCGTAGACCGTGCACCATG-3' and antisense primer 5'-AAGAATTCTTAGGCATAAGCCTGCCGGGGCA-3'. Core to NS2 coding region of JFH-1 was amplified using pJFH-1 as a template and sense primer 5'-GAGAATTCGTAGACCGTGCACCATG-3' and antisense primer 5'-AAGAATTCTTAAAGGAGCTTCCACCCCTTGG-3'. Amplified fragments were inserted into EcoRI site of pEF4 (Invitrogen) to generate pEFJFH/c-p7 and pEFJFHc-NS2, respectively.

Establishment of cell lines capable of packaging JFH-1 replicon RNA into VLPs. Huh7 cells were transfected using Lipofectamine (Invitrogen) with either pEFJFH/c-p7 or pEFJFHc-NS2 and were cultured with 0.2 mg/ml of zeocin (Invitrogen). Zeocin-resistant colonies were collected 3 weeks after transfection. The cell lines, Huh/c-p7 and Huh/c-NS2 (expressing pEFJFH/c-p7 and pEFJFHc-NS2, respectively) were then electroporated with 1 μg of JFH-1 subgenomic replicon (SGR-JFH1) RNA and were cultured with 0.375 mg/ml of G418 (Nacalai Tesque). Expression of core, E2 and NS5A was confirmed by Western blotting using anti-HCV core and anti-HCV E2 monoclonal antibodies [22] and anti-HCV NS5A polyclonal antibody [23]. The total RNA of culture media for each cell line (Huh/c-p7/SGR and Huh/p-NS2/SGR) was extracted using the QIAampViral RNA Mini spin column (Qiagen). Real-time RT-PCR was performed using TaqMan EZ RT-PCR Core Reagents (PE Applied Biosystems), as described previously [24,25]. The HCV core antigen in the culture media was measured by immunoassay (Ortho HCV-Core ELISA Kit; Ortho-Clinical Diagnostics), following the manufacturer's instructions. Culture medium was centrifuged at 8000g for 30 min to remove all cellular debris, after which the supernatant was concentrated to 1 ml by centrifugation using Amicon Ultracel 100k (Amicon). The concentrated medium was then layered on top of a continuous 10–60% (wt/wt) sucrose gradient in phosphate buffered saline (PBS) and then centrifuged at 40,000 rpm at 4 ℃ for 16 h (SW41E rotor, Beckman). Fractions (1 ml each) were collected from the top of the tube (12 fractions in total) and the density for each fraction was determined. The concentrations of replicon RNAs and core proteins of each fraction were measured as described above.

Infectivity of HCV-LPs. To determine whether these cell lines produced infectious HCV-LPs, we performed a colony formation assay using neomycin-resistant gene of SGR-JFH1 RNA. Naive Huh7 cells were infected with pooled fractions of 1.12–1.20 g/ml of both cell lines and were cultured for 3 weeks with G418 at 0.375 mg/ml. Formed colonies were stained with crystal violet and counted.

We also performed an immunofluorescence study in order to analyze the infectivity of the HCV-LPs. Following 3 days of incubation, the cells were fixed and immunostained for NS5A with anti-NS5A rabbit polyclonal antibody as described previously (Murakami et al., in press). Ffu (focus forming units) was calculated essentially based on the method as described previously [7,26]. Virus titration was performed by seeding Huh-7 cells in 96-well plates at 1×10^4 cells/well. Samples were serially diluted 5-fold in complete growth medium and used to infect the seeded cells (six wells per dilution). Nuclei were labeled with 4',6-diamidino-2-phenylindole (DAPI).

Results

Establishment of cell lines capable of packaging JFH-1 replicon RNA into VLPs

Stable cell lines expressing JFH-1 structural proteins were generated by transfecting with either pEFJFH/c-p7 or pEFJFHc-NS2. Zeocin-resistant colonies were collected 3 weeks after transfection and the expression of JFH-1 structural proteins was confirmed by Western blotting using anti-HCV core and anti-HCV E2 monoclonal antibodies [22] (Fig. 1A, lanes 1 and 2). The cell lines, Huh/c-p7 and Huh/c-NS2 (expressing pEFJFH/c-p7 and pEFJFHc-NS2, respectively) were then electroporated with 1 μg of SGR-JFH1 RNA. Six G418-resistant colonies were selected 3 weeks after electroporation and were termed Huh/c-p7/SGR (1–6) and Huh/c-NS2/SGR (1–6) cells. Expression of core, E2 and NS5A of Huh/c-p7/SGR-1, and Huh/c-NS2/SGR-3 was confirmed by Western blotting (Fig. 1A, lanes 3 and 4).

To investigate whether HCV-LPs were secreted from Huh/c-p7/SGR and Huh/c-NS2/SGR cells, we analyzed the culture medium of these cell lines 6 days postinfection. As shown in Fig. 1B, HCV replicon RNA and core protein were secreted from both cell lines. Fifty milliliters of culture medium from one Huh/c-NS2/SGR-1 and Huh/c-p7/SGR-3 cell line was concentrated, layered on top of a continuous 10–60% (wt/vol) sucrose gradient in PBS and then centrifuged at 40,000 rpm at 4 ℃ for 16 h. Fractions were collected from the top of the tube and the concentrations of replicon RNAs and core proteins of each fraction were measured. HCV RNA and core protein were predominantly detected in the 1.15–1.20 g/ml fractions, with a peak fraction of 1.16 g/ml fraction (Fig. 2A). HCV-LPs were
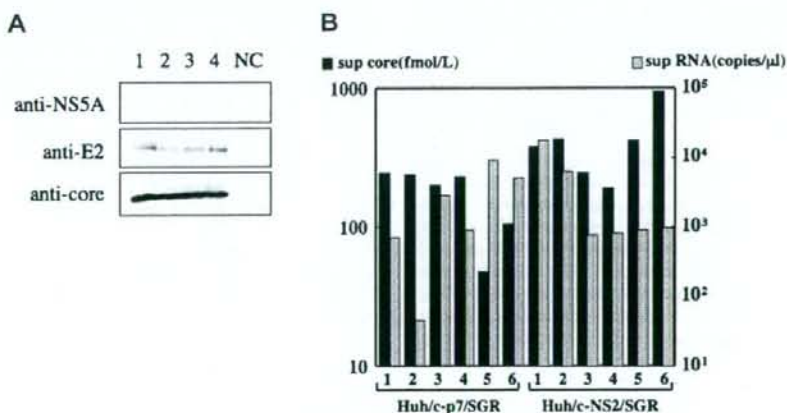
Fig. 1. (A) Western blot analysis of established cell lines. Huh/c-p7/SGR (1), Huh/c-NS2/SGR (2), Huh/c-p7/SGR-1 (3), and Huh/c-NS2/SGR-3 (4) cells were analyzed using anti-core, anti-E2, and anti-NS5A antibodies, respectively. Huh7 cells were used as a negative control. (B) Screening of G418-resistant cell lines. HCV replicon RNA and core protein of culture media of six colonies from Huh/c-p7/SGR or Huh/c-NS2/SGR cells were measured by real-time RT-PCR and ELISA, respectively. Black bars represented the concentration of core protein (fmol/l), dotted bars represented the concentration of replicon RNA (copies/μl).

observed by electron microscopy and these resembled previously reported particles (Fig. 2B)[27]. The secretion of HCV-LPs from these cell lines was maintained at almost the same level for more than 1 year (data not shown).

Infectivity of HCV-LPs

To determine whether these cell lines produced infectious HCV-LPs, we performed a colony formation assay using neomycin-resistant gene of SGR-JFH1 RNA. If HCV-LPs were infectious, SGR-JFH1 that was encapsidated in the particles would be introduced into infected cells, thus would confer neomycin resistance to the cells. To exclude the possibility that subgenomic replicon RNA in culture medium was captured by inoculated cells, Huh7 cells were also inoculated with concentrated culture medium of SGR-JFH1 cells. As shown in Fig. 3A, Huh7 cells infected with the fraction of Huh/c-NS2/SGR cells formed visible colonies 10–14 days after infection. Calculated colony forming units (cfu) of the culture medium of Huh/c-NS2/SGR cells were in the order of $5.54 \pm 2.92 \times 10^1$ cfu/ml similar to those of culture medium of JFH-1-infected cells [28]. The cells inoculated with concentrated medium of SGR-JFH1 cells formed no colonies (Fig. 3A). On the other hand, cells infected with Huh/c-p7/SGR formed no colonies, suggesting that NS2 protein was required for the infectivity of HCV-LPs. Infectivity of HCV-LPs from other cell lines of Huh/c-NS2/SGR, shown in Fig. 1, were also confirmed by colony formation assay, whereas HCV-LPs from other cell lines of Huh/c-p7/SGR showed no infectivity (data not shown).

In order to analyze the infectivity of the HCV-LPs, an immunofluorescence study was also performed. Huh7 cells infected with the Huh/c-NS2/SGR culture medium peak fraction (Fig. 2A) were positive for NS5A at 72 h postinfection (Fig. 3B), whereas the cells infected with the Huh/c-p7/SGR culture medium peak fraction

were negative for NS5A (Fig. 3B), suggesting that the expression of NS2 protein in infected cells was critical for the infectivity of the HCV-LPs. The infectivity of the Huh/c-NS2/SGR culture medium was calculated to be $3.4 \pm 0.6 \times 10^2$ ffu/ml. The Cfu of this culture medium was determined to be approximately 16% of ffu, likely because only a portion of introduced replicon could render neomycin resistance to the infected cells. The cells infected with JFH-1 showed spread of infection 72 h postinfection. On the other hand, the cells infected with the Huh/c-NS2/SGR culture medium peak fraction showed very limited or no spread of infection (Fig. 3B). Moreover, no NS5A-positive cells were observed when we inoculated new Huh7 cells with the concentrated culture medium from Huh7 cells that were infected the Huh/c-NS2/SGR culture medium peak fraction (Fig. 3B, reinfection), suggesting that HCV-LPs produced by Huh/c-NS2/SGR cells supported only a single-round of infection.

We also measured the infectivity of the 12 sucrose density gradient fractions of the culture medium of Huh/c-NS2/SGR cells. The density of the peak of infectivity was lower than the peak densities of the core protein and replicon RNA (Fig. 2A), however this result agreed with a previous observation [29].

Neutralization of HCV-LPs infection by CD81-specific antibody

CD81 was shown to be involved in HCV entry. To determine whether HCV-LPs formed in Huh/c-NS2/SGR cells were infected in a CD81-dependent fashion, we incubated Huh7 cells with the peak fractions of Huh/c-NS2/SGR and Huh/c-p7/SGR cells in the presence of 10 µg/ml of CD81 specific monoclonal antibody or nonspecific mouse antibody and cultured in the presence of 0.375 mg/ml of G418. After 3 weeks postinfection, colonies were fixed and the numbers of colonies were counted. CD81-specific antibody reduced the number of colonies from 132.3 ± 32.3 to 13.0 ± 11.5 ffu/
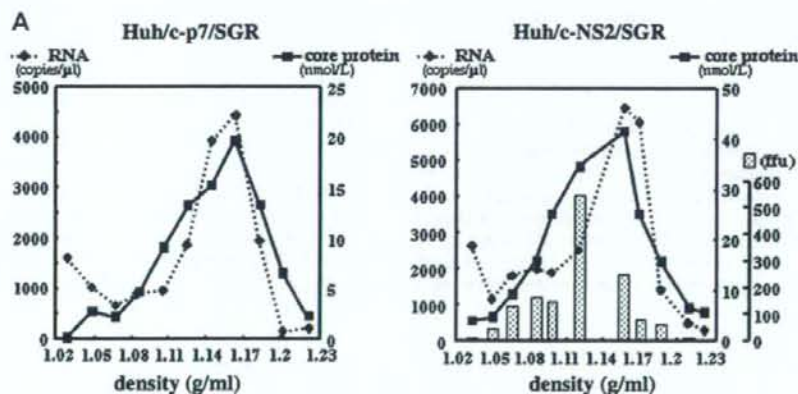
Fig. 2. (A) Sucrose density gradient analysis of culture supernatants of Huh/c-p7/SGR and Huh/c-NS2/SGR cells. Fifty milliliters of culture media collected from Huh/c-p7/SGR or Huh/c-NS2/SGR cells was concentrated to 1 ml and fractionated by ultracentrifugation at 40,000 rpm for 16 h by continuous 10–60% (wt/vol) sucrose gradient in PBS. Fractions (1 ml each) were collected from the top of the tube (12 fractions in total). HCV replicon RNA and core protein were measured by real-time RT-PCR and ELISA. The infectivity of each fraction of culture supernatant of Huh/c-NS2/SGR cells (right, lower panel) was determined by immunostaining of NS5A. (B) Electron microscopy analysis. Samples were prepared from the 1.12–1.20 g/ml fractions of culture media collected from Huh/c-NS2/SGR cells. Bar: 50 nm.
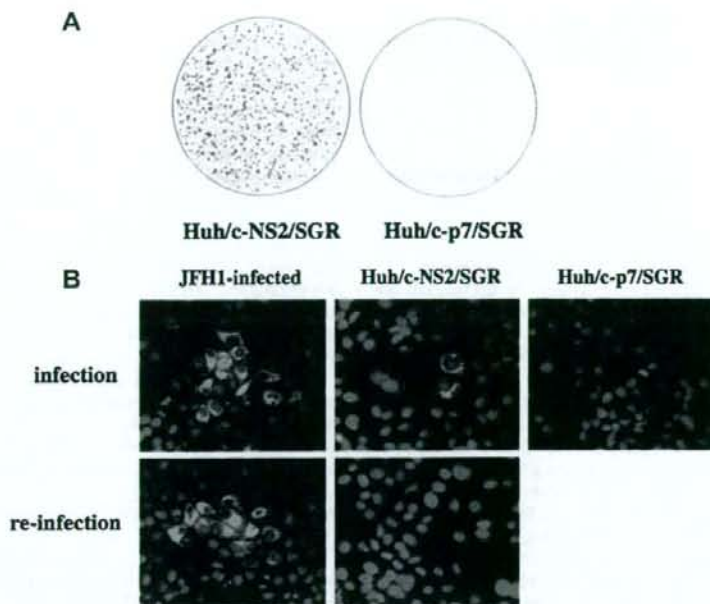
Fig. 3. (A) G418-resistant colony formation. Naive Huh7 cells were infected with 1.12–1.20 g/ml fractions of either Huh/c-p7/SGR or Huh/c-NS2/SGR cells and were cultured for 3 weeks with G418 at 0.375 mg/ml working concentration before staining with crystal violet. Experiments were performed in triplicate, and representative staining examples are shown. (B) Immunostaining experiments. Samples were serially diluted 5-fold in complete growth medium and used to infect the seeded cells (six wells per dilution). Huh7 cells in 96-well plates infected with the peak fraction of culture medium. Three days postinfection, infected cells were fixed, permeabilized with 0.3% Triton X-100 in Block Ace (Yukijirushi) and stained with anti-NS5A rabbit polyclonal antibody and Alexa488-conjugated goat anti-rabbit IgG as described previously (Murakami et al., in press). NS5A protein was shown in green. Nuclei were labeled with DAPI and were shown in blue. Re-infection shows the immunostaining of naive Huh7 cells infected with either culture media of JFH1-infected cells or that of Huh/c-NS2/SGR cells.

ml (Fig. 4), confirming that the infection of HCV-LPs to target cells is CD81-dependent and an important role of CD81 in HCV entry.

Discussion

Here we describe the development of cell lines selected to persistently harbor noncytopathic subgenomic replicons of HCV encoding neomycin resistant gene and the HCV core to NS2 cassette. The HCV-LPs secreted by this cell line are not proliferative and exhibit morphological, biophysical and antigenic properties similar to those of the putative HCV virions [27]. Jeong et al. suggested that HCV-LP is a potent immunogen for the induction of HCV-specific humoral and cellular immune responses by using

baboon as a primate model [30]. Recently, replicon-based vectors of positive-stranded RNA viruses were recognized as a desirable choice of highly efficient and safe vaccines. Recent comparative analyses of vaccine potential of Kunjin virus replicons delivered as plasmid DNA, as naked RNA, and as VLPs showed a significantly better induction of immune responses to an encoded immunogen after VLP delivery than with other delivery modalities [31]. These studies suggested that HCV-LPs encapsidating its subgenomic replicon RNA are an attractive candidate for a hepatitis C vaccine. We are now constructing cell lines that secrete HCV-LPs of genotype 1a and 1b strains with this trans-packaging system and analyzing the HCV-LPs infectivity. We also showed that the expression of NS2 region is essential for infectious
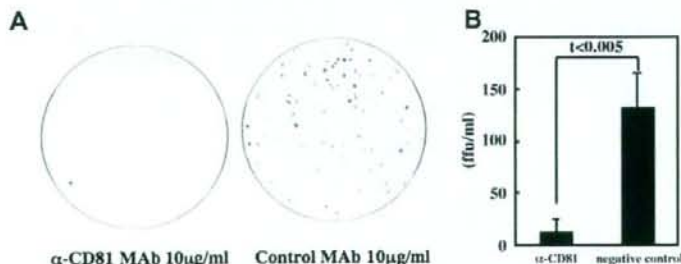
Fig. 4. Neutralization of HCV-LPs infection by CD81-specific antibody. Naive Huh7 cells were infected with peak fraction of either Huh/c-p7/SGR or Huh/c-NS2/SGR cells in the presence of 10 μg/ml of CD81 specific monoclonal antibody or nonspecific mouse antibody, then cultured 3 weeks with 0.375 mg/ml of G418. Colonies were stained with crystal violet and colony numbers were counted. (A) Colony formation. Experiments were performed in triplicate, and representative staining examples are shown. (B) Cfu of culture media per 1 ml was calculated and means ± SD was shown.

HCV-LPs production. NS2 is dispensable for RNA replication, since subgenomic replicons that lack the entire core to NS2 coding region replicate autonomously. The HCV NS2/3 protein is a highly hydrophobic protease responsible for the cleavage of the viral polypeptide between nonstructural proteins NS2 and NS3. However, many aspects of the NS2/3 protease's role in the viral life cycle and mechanism of action remain unknown. By using intergenotypic chimeras, Pietschmann et al. showed that NS2 plays an important role in the HCV morphogenesis by interacting with other NS proteins during the process of virion assembly [32]. Jones et al. reported that NS2 was required for infectious virus production and acts early in virion morphogenesis prior to the accumulation of infectious intracellular virus and indicated that the NS2 protease domain may form important interactions with other NS proteins during the process of virion assembly [33]. The results presented here also showed the importance of NS2 protein expression for the production of infectious particles, coincided with these previous observations. The mechanism NS2 plays in the process of virion morphogenesis is still unclear and remains to be determined.

In summary, we have generated a stable packaging cell line allowing production of large amounts of HCV-LPs in which the subgenomic replicon was encapsidated. The packaging cell line proved to be useful both for the production of HCV-LPs and for the encapsidation of HCV replicons for a single-round of infection.

Acknowledgments

References

[1] Q.L. Choo, K.H. Richman, J.H. Han, K. Berger, C. Lee, C. Dong, C. Gallegos, D. Coit, R. Medina-Selby, P.J. Barr, et al., Genetic organization and diversity of the hepatitis C virus, Proc. Natl. Acad. Sci. USA 88 (1991) 2451–2455.

[2] N. Kato, M. Hijikata, Y. Ootsuyama, M. Nakagawa, S. Ohkoshi, T. Sugimura, K. Shimotohno, Molecular cloning of the human hepatitis C virus genome from Japanese patients with non-A, non-B hepatitis, Proc. Natl. Acad. Sci. USA 87 (1990) 9524–9528.

[3] A. Takamizawa, C. Mori, I. Fuke, S. Manabe, S. Murakami, J. Fujita, E. Onishi, T. Andoh, I. Yoshida, H. Okayama, Structure and organization of the hepatitis C virus genome isolated from human carriers, J. Virol. 65 (1991) 1105–1113.

[4] A. Grakoui, C. Wychowski, C. Lin, S.M. Feinstone, C.M. Rice, Expression and identification of hepatitis C virus polyprotein cleavage products, J. Virol. 67 (1993) 1385–1395.

[5] M. Hijikata, N. Kato, Y. Ootsuyama, M. Nakagawa, K. Shimotohno, Gene mapping of the putative structural region of the hepatitis C virus genome by in vitro processing analysis, Proc. Natl. Acad. Sci. USA 88 (1991) 5547–5551.

[6] M. Hijikata, H. Mizushima, Y. Tanji, Y. Komoda, Y. Hirowatari, T. Akagi, N. Kato, K. Kimura, K. Shimotohno, Proteolytic processing and membrane association of putative nonstructural proteins of hepatitis C virus, Proc. Natl. Acad. Sci. USA 90 (1993) 10773–10777.

[7] B.D. Lindenbach, M.J. Evans, A.J. Syder, B. Wolk, T.L. Tellinghuisen, C.C. Liu, T. Maruyama, R.O. Hynes, D.R. Burton, J.A. McKeating, C.M. Rice, Complete replication of hepatitis C virus in cell culture, Science 309 (2005) 623–626.

[8] J. Zhong, P. Gastaminza, G. Cheng, S. Kapadia, T. Kato, D.R. Burton, S.F. Wieland, S.L. Uprichard, T. Wakita, F.V. Chisari, Robust hepatitis C virus infection in vitro, Proc. Natl. Acad. Sci. USA 102 (2005) 9294–9299.

[9] T.F. Baumert, S. Ito, D.T. Wong, T.J. Liang, Hepatitis C virus structural proteins assemble into virus like particles in insect cells, J. Virol. 72 (1998) 3827–3836.

[10] H.J. Ezelle, D. Markovic, G.N. Barber, Generation of hepatitis C virus-like particles by use of a recombinant vesicular stomatitis virus vector, J. Virol. 76 (2002) 12325–12334.

[11] E. Blanchard, D. Brand, S. Trassard, A. Goudeau, P. Roingeard, Hepatitis C virus-like particle morphogenesis, J. Virol. 76 (2002) 4073–4079.

[12] A.A. Khromykh, M.T. Kenney, E.G. Westaway, Trans-complementation of flavivirus RNA polymerase gene NS5 by using Kunjin virus replicon-expressing BHK cells, J. Virol. 72 (1998) 7270–7279.

[13] A.A. Khromykh, A.N. Varnavski, E.G. Westaway, Encapsidation of the flavivirus Kunjin replicon RNA by using replicon vectors providing Kunjin virus structural proteins in trans, J. Virol. 72 (1998) 5967–5977.

[14] T.J. Harvey, I. Anraku, R. Linedale, D. Harrich, J. Mackenzie, A. Suhrbier, A.A. Khromykh, Kunjin virus replicon vectors for human immunodeficiency virus vaccine development, J. Virol. 77 (2003) 7796–7803.

[15] C.T. Jones, C.G. Patkar, R.J. Kuhn, Construction and applications of yellow fever virus replicons, Virology 331 (2005) 247–259.

[16] R. Gehrke, M. Ecker, S.W. Aberle, S.L. Allison, F.X. Heinz, C.W. Mandl, Incorporation of tick-borne encephalitis virus replicons into virus-like particles by a packaging cell line, J. Virol. 77 (2003) 8924–8933.

[17] S.L. Hanna, T.C. Pierson, M.D. Sanchez, A.A. Ahmed, M.M. Murtadha, R.W. Doms, N-linked glycosylation of West Nile virus envelope proteins influences particle assembly and infectivity, J. Virol. 79 (2005) 13262–13274.

[18] F. Puig-Basagoiti, T.S. Deas, P. Ren, M. Tilgner, D.M. Ferguson, P.Y. Shi, High-throughput assays using a luciferase-expressing replicon, virus-like particles, and full-length virus for West Nile virus drug discovery, Antimicrob. Agents Chemother. 49 (2005) 4980–4988.

[19] T.J. Harvey, W.J. Liu, X.J. Wang, R. Linedale, M. Jacobs, A. Davidson, T.T. Le, I. Anraku, A. Suhrbier, P.Y. Shi, A.A. Khromykh, Tetracycline-inducible packaging cell line for production of flavivirus replicon particles, J. Virol. 78 (2004) 531–538.

[20] T.C. Pierson, M.D. Sanchez, B.A. Puffer, A.A. Ahmed, B.J. Geiss, L.E. Valentine, L.A. Altamura, M.S. Diamond, R.W. Doms, A rapid and quantitative assay for measuring antibody-mediated neutralization of West Nile virus infection, Virology 346 (2006) 53–65.

[21] T. Kato, T. Date, M. Miyamoto, A. Furusaka, K. Tokushige, M. Mizokami, T. Wakita, Efficient replication of the genotype 2a hepatitis C virus subgenomic replicon, Gastroenterology 125 (2003) 1808–1817.

[22] M. Shirakura, K. Murakami, T. Ichimura, R. Suzuki, T. Shimoji, K. Fukuda, K. Abe, S. Sato, M. Fukasawa, Y. Yamakawa, M. Nishijima, K. Moriishi, Y. Matsuura, T. Wakita, T. Suzuki, P.M. Howley, T. Miyamura, I. Shoji, E6AP ubiquitin ligase mediates ubiquitylation and degradation of hepatitis C virus core protein, J. Virol. 81 (2007) 1174–1185.

[23] K. Murakami, T. Kimura, M. Osaki, K. Ishii, T. Miyamura, T. Suzuki, T. Wakita, I. Shoji, Virological characterization of HCV JFH-1 strain in lymphocytes, J. Gen. Virol. (in press).

[24] H. Aizaki, K.J. Lee, V.M. Sung, H. Ishiko, M.M. Lai, Characterization of the hepatitis C virus RNA replication complex associated with lipid rafts, Virology 324 (2004) 450–461.

[25] T. Suzuki, K. Omata, T. Satoh, T. Miyasaka, C. Arai, M. Maeda, T. Matsuno, T. Miyamura, Quantitative detection of hepatitis C virus (HCV) RNA in saliva and gingival crevicular fluid of HCV-infected patients, J. Clin. Microbiol. 43 (2005) 4413–4417.

[26] M. Yi, R.A. Villanueva, D.L. Thomas, T. Wakita, S.M. Lemon, Production of infectious genotype 1a hepatitis C virus (Hutchinson strain) in cultured human hepatoma cells, Proc. Natl. Acad. Sci. USA 103 (2006) 2310–2315.

[27] T. Wakita, T. Pietschmann, T. Kato, T. Date, M. Miyamoto, Z. Zhao, K. Murthy, A. Habermann, H.G. Krausslich, M. Mizokami, R. Bartenschlager, T.J. Liang, Production of infectious hepatitis C virus in tissue culture from a cloned viral genome, Nat. Med. 11 (2005) 791–796.

[28] T. Date, M. Miyamoto, T. Kato, K. Morikawa, A. Murayama, D. Akazawa, J. Tanabe, S. Sone, M. Mizokami, T. Wakita, An infectious and selectable full-length replicon system with hepatitis C virus JFH-1 strain, Hepatol. Res. 37 (2007) 433–443.

[29] Y. Miyanari, K. Atsuzawa, N. Usuda, K. Watashi, T. Hishiki, M. Zayas, R. Bartenschlager, T. Wakita, M. Hijikata, K. Shimotohno, The lipid droplet is an important organelle for hepatitis C virus production, Nat. Cell. Biol. 9 (2007) 1089–1097.

[30] S.H. Jeong, M. Qiao, M. Nascimbeni, Z. Hu, B. Rehermann, K. Murthy, T.J. Liang, Immunization with hepatitis C virus-like particles induces humoral and cellular immune responses in nonhuman primates, J. Virol. 78 (2004) 6995–7003.

[31] I. Anraku, T.J. Harvey, R. Linedale, J. Gardner, D. Harrich, A. Suhrbier, A.A. Khromykh, Kunjin virus replicon vaccine vectors induce protective CD8+ T-cell immunity, J. Virol. 76 (2002) 3791–3799.

[32] T. Pietschmann, A. Kaul, G. Koutsoudakis, A. Shavinskaya, S. Kallis, E. Steinmann, K. Abid, F. Negro, M. Dreux, F.L. Cosset, R. Bartenschlager, Construction and characterization of infectious intragenotypic and intergenotypic hepatitis C virus chimeras, Proc. Natl. Acad. Sci. USA 103 (2006) 7408–7413.

[33] C.T. Jones, C.L. Murray, D.K. Eastman, J. Tassello, C.M. Rice, Hepatitis C virus p7 and NS2 proteins are essential for production of infectious virus, J. Virol. 81 (2007) 8374–8383.

ORIGINAL PAPER

Identification and characterization of the human inhibitor of caspase-activated DNase gene promoter

Kazuhiko Omata · Ryosuke Suzuki · Takahiro Masaki ·
Tatsuo Miyamura · Tazuko Satoh · Tetsuro Suzuki

Abstract DNA fragmentation factor is a heterodimer complex of the nuclease CAD and its specific inhibitor ICAD, which can be activated during apoptosis to induce DNA fragmentation. Although ICAD expression levels have been quantified in a variety of human cancer cells, the mechanism of ICAD gene regulation remains unknown. In this study, we identified a 106-bp TATA-less region upstream of the transcription start site as a basal promoter of the human *ICAD* gene. An E-Box motif, which binds transcription factors of the basic helix-loop-helix/leucine zipper family, is responsible for transcriptional activity, as demonstrated using mutated promoter-reporters. A chromatin immunoprecipitation assay further demonstrated that Myc binds to an endogenous *ICAD* promoter. The functional importance of Myc in the regulation of *ICAD* transcription was also demonstrated by knock-down of *c-Myc* and *N-Myc* gene expression, as well as their ectopic expression. Structural analysis of the human *ICAD* promoter and identification of factors which regulate its activity might further our understanding of the biological role of ICAD with respect to regulation of apoptosis and cancer development.

Keywords ICAD · DFF · Promoter · Gene expression · Myc

K. Omata · R. Suzuki · T. Masaki · T. Miyamura ·
T. Suzuki (✉)
Department of Virology II, National Institute of Infectious
Diseases, 1-23-1 Toyama, Shinjuku-ku, Tokyo, Japan
e-mail: tesuzuki@nih.go.jp

K. Omata · T. Satoh
Department of Oral and Maxillofacial Surgery, School of Life
Dentistry at Tokyo, The Nippon Dental University, Tokyo, Japan

Introduction

Apoptosis or programmed cell death ensures the elimination of unwanted cells during normal development and homeostasis [1]. This process is progressively inactivated during malignant development and loss of the capacity for apoptosis is a hallmark of malignant cells. Chromatin condensation and internucleasomal DNA fragmentation are typical nuclear features and well-recognized events in apoptosis. DNA fragmentation factor (DFF) is a heterodimer protein composed of a 40-kDa caspase-activated DNase (CAD) otherwise known as DFF40, and its cognate 45-kDa inhibitor (inhibitor of CAD: ICAD or DFF45 [2–8]). Both human genes map to 1p36 [9, 10]. CAD is thought to be responsible for the majority of nuclear activity resulting in chromosomal DNA fragmentation. When apoptosis is activated, ICAD is cleaved by executor caspases, mainly caspase-3, into three fragments, after which it dissociates from CAD, resulting in CAD activation.

Thus, the DFF complex may play a role in malignant transformation, and up- or down-regulation of ICAD/CAD expression might correlate with cancer aggression. Expression levels of ICAD have been examined in a variety of human cancers. For example, ICAD expression is down-regulated during the exponential growth phase of human colon carcinoma cells [11]. In some neuroblastomas, preferential ICAD expression is observed in low-stage, but not in their high grade [12]. Other research suggests that down-regulation of ICAD may contribute to tumor growth and lymph node metastasis in esophageal carcinoma [13], and that ICAD expression might serve as a marker of aggressive tumor behavior with an associated poor prognosis in ovarian cancer [14]. We have previously demonstrated that the hepatitis C virus core protein, which not only encodes the viral nucleocapsid but has a number of properties enabling

persistent viral infection, induces gene expression of *ICAD*, thereby increasing steady-state levels of the ICAD protein [15]. To date, the mechanism of transcriptional regulation of the *ICAD* gene is not well understood. Analysis of the gene structure of mouse *ICAD* showed that a 118-bp flanking region of the *ICAD* gene is required for promoter activity [16]. In this study, we identified a functional promoter of the human *ICAD* gene and investigated the role of c-Myc and N-Myc in regulation of the *ICAD* promoter.

Materials and methods

Cell cultures

Human hepatoblastoma cells (Huh-7), human oral squamous carcinoma cells (HSC-2, HSC-3 and Ca22-9), mouse neuroblastoma cells (IMR-32 and GOTO) and mouse 3T3 cells were maintained in Dulbecco's modified Eagle's medium (DMEM) supplemented with 10% fetal bovine serum, 100 units/ml of penicillin, and 100 mg/ml of streptomycin and kept at 37°C in a 5% CO_2 incubator.

Cloning of the 5'-upstream region of the human *ICAD* gene

Human genomic DNA was isolated from Huh-7 cell lines using the QIAamp DNA Mini kit according to the manufacturer's instructions (QIAGEN). A 5'-upstream region of the *ICAD* gene was amplified by PCR using primers based on the genomic DNA sequence of the human *ICAD* gene (GenBank accession No. NM_004401). Primers containing *EcoRI* sites were used as follows: forward (5'-GA-ATTCAGGCTGGTCTCAAACTACTG-3') and reverse (5'-GAATTCGATCTCGCCAGATTCTGGTA-3'). The PCR reaction was carried out at 94°C for 1 min, 55°C for 1.5 min, and 72°C for 2 min, for total of 35 cycles. Each PCR product was purified and subcloned into a pGEM-T Easy vector (Promega), followed by sequencing using an ABI PRISM 310 automated DNA sequencer (Applied Biosystems).

5' rapid amplification of cDNA ends (5'-RACE) assay

The 5' ends of the *ICAD* transcript were cloned by 5'-RACE using a Gene Racer RACE-Ready cDNA kit in accordance with the manufacturer's instructions (Invitrogen). Double-stranded cDNA molecules prepared from human liver poly(A)$^+$ RNAs ligated by exposure to the adaptor were amplified in a primary PCR reaction using the adaptor primer 1 and the *ICAD* gene-specific antisense primer ICA1AS (5'-GTGCTGTTCGCGGCTGTAGTT-3', nt −147 to −173), followed by a secondary PCR reaction

using nested oligonucleotides, the adaptor primer 2, and the antisense *ICAD* specific primer ICA2AS (5'-CACGG TGACTGGTGTCAGGGACTTATC-3', nt −228 to −254). PCR products were purified and cloned, followed by nucleotide sequencing as described above.

Plasmid constructions

The 1-kb sequence containing the human *ICAD* promoter was excised by digestion of the above-mentioned pGEM-T vector with *SacI* and *Hind*III, and then cloned into the firefly-luciferase-expressing reporter plasmid pGL3-Basic (Promega), resulting in pLUC1005. A series of constructs with 5' end-deletions of the *ICAD* promoter were created by PCR amplification using the reverse primer (5'-CAA GCTTGCCTCCACAAGGTGGGACCTG-3') and the following forward primers: 5'-GGCTAGCCAGTACCCATTT CTGAAGAAG-3' (nt −936 to +71), 5'-GGCTAGCCCTCA TTTGGGTCCATTTTCC-3' (nt −622 to +71), 5'-GGCTAG CCAGCTTTTTCAGACAGAATGG-3' (nt −272 to +71), 5'-GGCTAGCCAGCTTTTTCAGACAGAATGG-3' (nt −205 to +71), 5'-GGCTAGCCAGCTTTTTCAGACAGAATGG-3' (nt −145 to +71), 5'-GGCTAGCCAGCTTTTTCAGACA GAATGG-3' (nt −106 to +71), 5'-GGCTAGCCTATTTA GTTTGGTTAGTAAT-3' (nt −90 to +71), and 5'-GGCTAG CCCAGATGGTAAATATACACAA-3' (nt −43 to +71). Each *SacI/Hind*III fragment was inserted into the pGL3-basic vector to yield pLUC(−936/+71), pLUC(−622/+71), pLUC(−272/+71), pLUC(−205/+71), pLUC(−145/+71), pLUC(−106/+71), pLUC(−90/+71) and pLUC(−43/+71).

Transfection and reporter assay

Huh-7 cells were seeded at 5×10^4 cells/well in 24-well plates and maintained at 37°C in a 5% CO_2/95% atmosphere. DNA transfection of cells with each *ICAD*-promoter-luciferase construct (1 μg) with an internal control vector pRL-TK (0.1 μg) (Promega) was performed with Trans IT LT-1 (Mirus) during 6-h of incubation. Cells were then rinsed with phosphate-buffered saline (PBS) 48 h after transfection, and luciferase activity was measured in the cell lysate using dual luciferase assay reagents (Promega) [17]. Firefly luciferase activity was standardized according to Renilla luciferase activity.

Chromatin immunoprecipitation

Chromatin immunoprecipitation assays were performed using the ChIP assay kit (Upstate). Briefly, cells in 100-mm dishes were grown to 70% confluency over 48 h. The chromatin from formaldehyde-fixed cells was sonicated and immunoprecipitated using mouse monoclonal anti-c-Myc or anti-N-Myc antibodies (Santa Cruz). The chromatin immunoprecipitate

was analysed by PCR with the following primer pairs: F1 (5′-CGAGCTCGGTATACATGCGTGTGCATCG-3′) and R1 (5′-CAAGCTTGCCTCCACAAGGTGGGACCTG-3′) for amplifying the region from nt −272 to −71 containing potential Myc-binding sites; and F2 (5′-GAGATCAAAAC TGCAGTGAG-3′) and R2 (5′-CACTGTTGGAGATTGTT CAG-3′) for amplifying the region from nt −789 to −451 that does not contain Myc-binding sites.

Western blotting

Cells were washed with PBS and lysed in SDS sample buffer. Cell lysate samples were separated by 10% SDS-polyacryl-amide gel electrophoresis and electrotransferred to a polyvinylidene difluoride membrane (Immobilion; Millipore). After blocking in nonfat milk solution (Blocking One; Nakaraitesk), the membranes were probed with mono-clonal antibody against the ICAD protein (Santa Cruz), c-Myc (Sigma), or N-Myc (Santa Cruz), as the primary antibody for 1 h. After being washed, the membranes were incubated with horseradish peroxidase-conjugated anti-mouse immunoglobulin as the secondary antibody, followed by visualization with SuperSignal West Pico Chemilumi-nescent Substrate (Pierce Biotechnology).

siRNA experiments

siRNAs for human c-Myc, N-Myc and the negative control were purchased from B-Bridge International. Each siRNA consisted of three different target sequences as follows: 5′-GAGGAGACAUGGUGAACCA-3′ 5′-GAGAAUGUCA AGAGGCGAA-3′, and 5′-GAGAAUGUCAAGAGGCGAA -3′ for c-Myc siRNA; 5′-CGGAGAUGCUGCUUGAGAA-3′, 5′-CGGAGUUGGUAAAGAAUGA-3′, and 5′-CAGCAGU UGCUAAAGAAAA-3′ for N-Myc siRNA; and 5′-ATCC GCGCGATAGTACGTA-3′, 5′-TTACGCGTAGCGTAAT ACG-3′, and 5′-TATTCGCGCGTATAGCGGT-3′ for the negative control. Huh-7 cells were transfected with 100 pmol/ml siRNA using FuGENE6 (Roche) in Opti-MEM I (Invitro-gen), after which the medium was replaced by standard DMEM after 6 h of transfection.

RNA preparation and real-time quantitative RT-PCR

Total RNA was extracted using Trizol reagent (Invitrogen) according to the manufacturer's protocol. First-strand cDNAs were synthesized using the SuperScriptIII First-Strand Synthesis kit (Invitrogen) and then used as templates for real-time PCR. Quantitative PCR was performed using the ABI Prism 7700 sequence detection system using Taq-Man Gene Expression assays (Applied Biosystems). The standard curve was created using serially diluted total RNA obtained from Huh-7 cultures and β-actin was chosen as the

internal standard to control for variability in amplification. Amplification was performed at 95°C for 10 min, followed by 40 cycles of amplification at 95°C for 15 s and 60°C for 60 s.

Results and discussion

Localization of transcription start sites of the human ICAD gene

Precise localization of transcription start sites of the ICAD gene was examined in human hepatoma Huh-7 cells by 5′-RACE analysis. A fragment of approximately 100 bp was obtained (Fig. 1a) and cloned, after which sequencing analysis of sev-eral cDNA clones identified two of 5′ termini (Fig. 1b). These were located 71 and 68 nucleotides upstream from the trans-lation start codon of the ICAD gene. From a database search of the DBTSS [18], we found that these are two of multiple sites for putative transcription initiation for the human ICAD gene. Although transcription may be initiated at both sites, the upper site was designated position +1 in this study.

Characterization of the ICAD gene promoter

To examine potential regulatory sequences involved in ICAD gene expression, a 1 kb 5′-upstream region of the ICAD gene was sequenced and analyzed. The overall GC content of the 1-kb genomic DNA fragment was 46%, while GC content among the 200 bp proximal to the ATG start codon was approximately 62%. A search of tran-scription consensus motifs using the TRANSFAC database [19] demonstrated that none of the major eukaryotic pro-moter elements, TATA-, CCAAT-, or GC box, were located within 200 bp upstream of the transcription start site, although a TATA-like element was found more than 400 bp upstream from the start sites, indicating that the human ICAD gene has a TATA-less promoter. No CpG island, which is frequently observed in the TATA-less promoter, was found by screening with the CpG island searcher (http://cpgislands.usc.edu/). Absence of a TATA-like sequence upstream of the transcription start site has also been reported for the mouse ICAD gene, suggesting that TATA-less promoters might be a common feature in transcriptional regulation of the ICAD gene.

As shown in Fig. 1b, the 1-kb sequence contains potential binding sites for several transcription factors. The ability of the 5′-upstream region of the ICAD gene to function as a promoter was assessed by its capacity to drive the expression of a luciferase reporter gene. A series of constructs in which genomic DNA fragments were fused to a promoterless firefly luciferase gene of the pGL3-basic vector were generated with the 3′ end always terminating +71 bp from the

Fig. 1 (a) Mapping of the transcription start sites by 5' RACE analysis. Following nested PCR reaction, a PCR product of 100-bp was detected by 1.5% agarose gel electrophoresis (lane 2). Lane 1: no template control; lane M: 100-bp DNA ladder marker. (b) The 5' flanking region of the human *ICAD* gene. The nucleotide sequence is numbered from the major transcription site, which is indicated by an arrow. Putative binding sites for transcription factors analyzed by the TRANSFAC database and search program were shown with underlines

A

M 1 2

B

```
-960                                        AGGCT GGTCTCAAAC TACTGACCTC AGATCATCTG -901
                                                       SRY      CRE-BP/CREB
-900 TCCGCCTCGG CCTCCTAAAG TGCTGAGATT ACAGGGGTGA GCCACCGCCC CCGGGGCCCT -841
                          Nkx-2
-840 TGCCCACGTT TTTATAAACA AAATATGAGG TGGGAGGATT GCTTGAGCCC AGGAGATCAA -781
          CdxA    SRY           AML1-a       GATA-2
-780 AACTGCAGTG AGCCATCATC GCGCCACTGC ACTCCAGCCT GGGAGACAGA GCGAAACGCT -721
-720 GTCTCAAAAA AAGAAAAAAG AAACAAGGAA GGAAAGTGTC CCCCGAATGA ATAAATATGA -661
                    SRY                                        Pbx-1   CdxA
-660 GCAGATAATT ACTTCTAGTT TACATAAAAT GCCCTCTTTT AAGAGAGGAA CTTTTTGATC -601
       GATA-1        CRE-BP/VBP
-600 ATTTTTATTA CTATTCTTTT AATCTTAGAT GTTTATTTTT CAGGAGGAAA AAAACAAACT -541
             CdxA                  HFH-2/HFH-1                        SRY
-540 TTTCCATAGT AGCAGTATTA AAACAAAGAT GAATATGTTG TCAAGAGGCA TCTGAACAAT -481
                          SRY                                    Sox-5/HSF2
-480 CTCCAACAGT GCCAGTCGC ATTTCCCCTT TCCTCTCCGA TGCATTTGAG ACTTTAATGC -421
-420 TTACTATATT TATTTAAGCG TTTTGTTCTG AGACCCCAAA CTAATTTGCA CAGTTGAAGC -361
         HFH-2    CdxA                          SRY       Oct-1
-360 AGGAAATAGA ATGGGTGGAA ACATGCGGGT GTCTGTATTA GCATTATGCA TCTCATATGC -301
       c-Ets                                          CdxA
-300 GAATAGGAAT GCTCTAAAAA TTCAATACAG TATACATGCG TGTGCATCGT CATGCAAAAT -241
           HFH-2                                             Brn-2
-240 AAGTCTCTAT TGGCCTTATA TTTGAACGCG CGAATGCAGC TCCTAAAAGT TAAAAACAAC -181
                                                                    SRY
-180 TCCTAGGCTG AATCGCGCGA TAGAACGAAA GCGGCTTTAA ACCCAGAGAC TACAGTTTCC -121
                       GATA-1
-120 GGCATGCTTC GACGCCACAC GTGATTAGCG GCAACTAGAA CTACATTTCC CGGCGTGCCC -61
         Myc/USF    GATA-1              HSF
-60  TGGTCTCACG TGTGATTTGC TGCGGAACGA ACTACATCTC CCGGCAGGCT GCGGAAGGGG -1
         Myc/USF
+1   GTCGAGTAGA AGGACCGCCG CTCCGGCCTC CCGCGACTTC TCGAAGGTGG GCAGGTCCCA +60
```

transcription start site. The 5' ends began at bases −936, −662, −272, −205, −145, −106, −90, and −43 (Fig. 2). Promoter activity was assessed by measuring luciferase activity in transiently transfected Huh-7 cells. Luciferase activity was normalized to Renilla luciferase activity. As shown in Fig. 2 on the right, the region extending from −936 to +71 had promoter activity since luciferase activity of the reporter gene was 45-fold that of the empty vector. A 5' deletion of the promoter sequence to −662(pLuc(−662/+71)) enhanced promoter activity, and successive removal of nucleotides from −272 to −106 also enhanced promoter activity, suggesting the possibility of negative regulatory elements within the −936/−622 and −272/−106 regions.

When the sequence from −106 to −90 was removed (pLuc(−90/+71)), promoter activity fell to parallel that of the pGL3 basic vector. This suggests the presence of a critical element in the region extending from −106 to −90, thus, we have identified the region 106 bp upstream of the transcription start site as the basal promoter of the human *ICAD* gene.

Myc and USF enhance *ICAD* promoter activity

As indicated in Fig. 1b, a computer-based sequence analysis revealed that the 106 bp region contains potential binding sites for GATA-1, deltaE, Myc, and various upstream stimulatory

Fig. 2 Human *ICAD* promoter drives reporter gene expression in transiently transfected Huh-7 cells. Deletion constructs of the upstream region of the *ICAD* gene linked to the firefly luciferase reporter gene (LUC) are illustrated in the left. Huh-7 cells were cotransfected with a firefly luciferase reporter and a Renilla luciferase internal control (pRL-TK). The relative luciferase activity (RLU) was obtained by normalizing the firefly luciferase activity to the Renilla luciferase activity, and is expressed as a percentage of RLU of pLuc(−936/+71). The average values are shown with standard deviation (SD) ($n = 4$ per construct)

factors (USF). Within this region, there is a canonical E-box sequence (5'-CACGTG-3') located between −103 and −98. E box motifs are known to bind to transcription factors of the basic helix-loop-helix/leucine zipper (bHLH LZ) family, including Myc and USF [20–23]. We examined the potential role of E-box-binding proteins, Myc and USF, in potentiating *ICAD* gene transcription. Myc is bound to a partner protein Max via a bHLH LZ domain and the Myc-Max heterodimer activates transcription by binding to an E-box sequence [24, 25]. Max is present in greater amounts than Myc since the Myc transcript and protein have shorter half-lives compared to Max [26, 27]. Therefore, it is highly likely that Myc is the limiting, regulated component of the heterodimer. To examine the potential role of E box binding proteins, Huh-7 cells were co-transfected with luciferase reporter plasmids and expression vectors for c-Myc, N-Myc, USF1, and USF2 (Fig. 3a). Luciferase activity of the −145/+71 promoter construct increased 2- to 5-fold, and 1.5- to 2-fold, when co-expressed with Myc or USF, respectively. The effect of c-Myc and N-Myc on activity of the −90/+71 construct was less than for the −145/+71 construct. USF expression did not enhance activity of the −90/+71 construct.

To further investigate involvement of the E box sequence in *ICAD* promoter activity, a reporter construct with an E box mutation (CCCGCG) was constructed and luciferase activity was examined in transfected cells (Fig. 3b). The E box mutation resulted in marked downregulation of reporter gene expression and the reporter activity expressed from the E-box mutant was little increased when co-expressed with Myc, suggesting a functionally important role of the −106/−90 region E box motif with regard to basal transcriptional activation of the *ICAD* promoter. These data indicates that E-box-binding proteins, especially Myc, actively participate in positive regulation of the human *ICAD* promoter.

Myc binds to the *ICAD* promoter in vivo

To obtain direct evidence of an interaction between Myc and the *ICAD* promoter in vivo, we next examined binding of c-Myc and N-Myc to the 5'-upstream region of the *ICAD* gene within the context of native chromatin in living cells by chromatin immunoprecipitation. An alignment of the sequence around putative Myc binding site of human *ICAD* promoter and the corresponding part of mouse *ICAD* sequence demonstrated conservation of Myc binding sequence in human and mouse (Fig. 4a) [16]. Proteins were cross-linked to genomic DNA isolated not only from human (Huh-7) but mouse (IMR-32 and GOTO) cells, followed by immunoprecipitation with normal rabbit IgG or polyclonal antibodies to either c-Myc or N-Myc. IMR-32 and GOTO are neuroblastoma cells with *N-Myc* gene amplification [28]. The precipitated DNA was then subjected to PCR utilizing
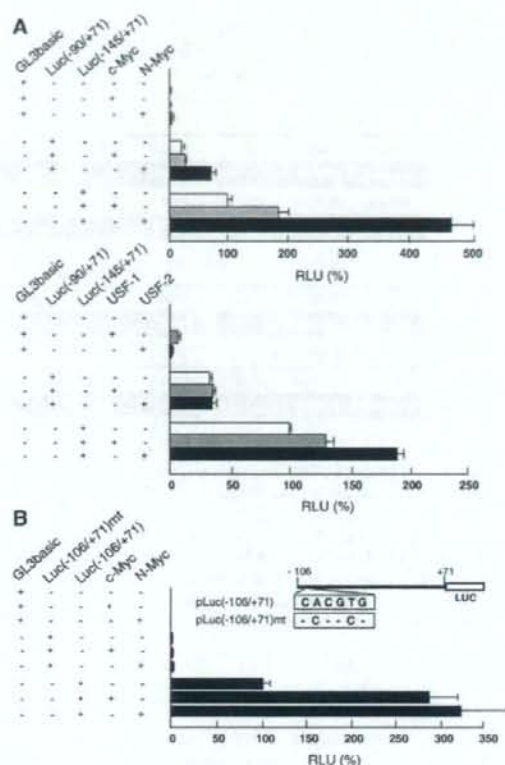
Fig. 3 (a) *ICAD* promoter activity after transient expression of c-Myc, N-Myc, USF1 and USF2. Huh-7 cells were cotransfected with either expression vector for c-Myc, N-Myc, USF1 or USF2 driven by the CMV promoter and pLuc(−145/+71), pLuc(−90/+71) or pGL3 basic. Each firefly luciferase reporter plasmid (*n* = 4) was cotransfected in cells with pRL-TK for normalization of the reporter activity. RLU is expressed as a percentage of that of pLuc(−145/+71) in the absence of expressing plasmids for Myc and USF. (b) Effect of substitution mutation in the E-box element on the *ICAD* promoter activity. Cells were cotransfected with pLuc(−106/±71) or an E-box-mutant, pLuc(−106/±71)mt and either expression vector for c-Myc or N-Myc. pRL-TK was also used for normalization of the activity. RLU is expressed as a percentage of that of pLuc(−106/±71) without over-expression of Myc

primers designed to amplify a 343-bp fragment (−272/+71) or a 338 bp fragment (−789/−451) of the *ICAD* 5' flanking region. As shown in Fig. 4b, the 343-bp DNA fragment was observed in the immunoprecipitate from Huh-7 cells following exposure to anti-c-Myc or anti-N-Myc, while amplification of the *ICAD* promoter fragment was not detected in the negative control immunoprecipitate. Under similar experimental conditions, we did not detect binding of c-Myc and N-Myc to the −789/−451 region, which is not thought to contain a Myc-binding site. Similar results were

A

| human | -101 CGCCACACGTGATTAGCGGCAACTAGAACT -72 |
| mouse | GAACGCCCGTGATTAGCCGCCACTAGAACT |

Myc/USF GATA-1   HSF

B
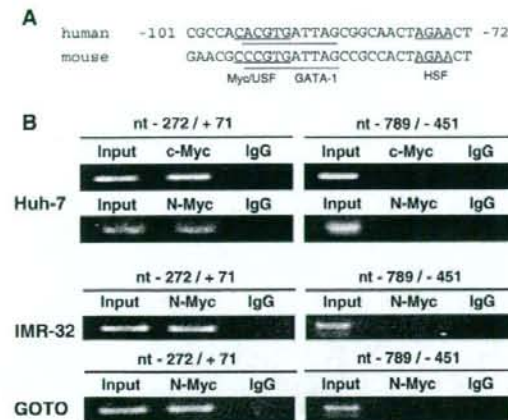
Fig. 4 (a) An alignment of the sequence around putative Myc binding site of human *ICAD* promoter and the corresponding part of mouse *ICAD* sequence. (b) Binding of Myc proteins in the endogenous *ICAD* promoter. Crosslinked chromatins isolated from Huh-7, IMR-32 and GOTO cells were immunoprecipitated with indicated antibodies (c-Myc, N-Myc) or an equivalent amount of mouse IgG. Recovered DNAs were purified and PCR-amplified with primers for nt −272/±71 region or for nt −789/−451 region. Input represents 1% of chromatin sample applied for immunoprecipitation

obtained from IMR-32 and GOTO cells, which were immunoprecipitated with anti-N-Myc antibody. These results demonstrate that Myc forms a complex with the human *ICAD* promoter in cells, presumably through binding to the E-box sequence.

Myc-dependent expression of the ICAD protein

The above data suggests that the *ICAD* promoter is regulated by endogenous Myc proteins. This assumption is supported by the loss-of-function studies shown in Fig. 5a. We employed siRNA (small interference RNA) transfection to knock-down the expression of c-Myc or N-Myc in cells, after which we analyzed the effect of reduced Myc expression on steady state levels of the ICAD protein by Western blotting. Treatment with siRNA specific for either c-Myc or N-Myc markedly reduced ICAD expression without affecting the expression of β-actin. In contrast, control siRNA did not reduce ICAD levels. We further investigated the effect of over-expression of Myc on ICAD protein levels (Fig. 5b). Transfection of Huh-7 and mouse 3T3 cells with a c-Myc or N-Myc expression vector enhanced ICAD protein levels with an effect that was less pronounced than in the
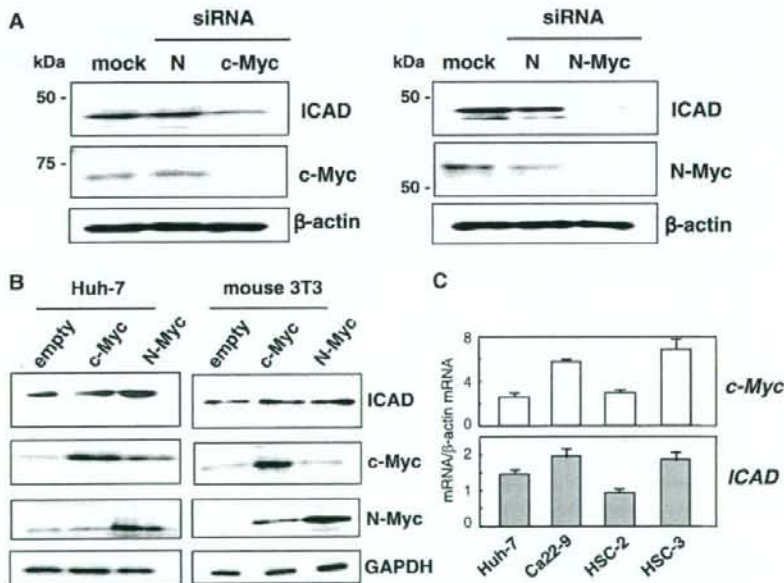
Fig. 5 Myc-dependent expression of human ICAD. (a) Suppression of Myc expression decreases expression of ICAD protein. Huh-7 cells were transiently transfected with Myc siRNA (c-Myc, N-Myc) or the control siRNA (cont). Three days later, the cells were harvested and subjected to Western blotting. (b) Ectopic expression of Myc increases expression of ICAD protein. Cells (Huh-7 and mouse 3T3) were transfected with the expression vector for c-Myc or N-Myc, and after 3 days the cells were harvested for Western blotting. (c) Comparison of the mRNA expression of *c-Myc* and *ICAD* in Huh-7 cells and human oral squamous carcinoma cells (Ca22-9, HSC-2, and HSC-3). Levels of mRNA expression of ICAD and c-Myc were measured by quantitative real-time RT-PCR based on Taq Man chemistry. Results, relative to β-actin mRNA, are depicted as averages with SD ($n = 3$)

935

loss-of-function studies, but reproducible nonetheless. These results suggest an important role of Myc proteins in positive regulation of ICAD expression.

Finally, we examined if there might be a correlation between *ICAD* and *Myc* expression levels in cancer cell lines. The mRNA expression of *ICAD* and *c-Myc* in human oral squamous cell carcinomas (Ca22-9, HSC-2, and HSC-3), in which *ICAD* expression has not been investigated to date, as well as in Huh-7 cells during their late exponential phase of growth, was analyzed by quantitative RT-PCR (Fig. 5c). *ICAD* mRNA was readily detected in all cancer cells but the expression level was not consistent. A relatively high level of expression was observed in Ca22-9 and HSC-3 cells, while HSC-2 cells demonstrated the lowest. Interestingly, expression pattern of *c-Myc* mRNA in these cell lines showed a tendency similar to that of ICAD, suggesting an important role of Myc in ICAD expression in human cancers. A large scale analysis for investigating correlation between ICAD and Myc expression in a variety of cancer tissues obtained from patients is ongoing.

Several studies have shown up- or down-regulation of ICAD in a variety of human cancers [11–14, 29, 30]. Although transcriptional deregulation is presumably involved in this aberrant expression of ICAD, little is known about the transcriptional regulation of *ICAD* in human cells. This work was done to characterize the human *ICAD* promoter and to examine transcription factors which may be involved in its regulation. We experimentally determined putative transcription start sites by employing the 5′-RACE method, and identified a promoter region required for basal *ICAD* gene expression using promoter-reporter constructs with progressive deletions. A combined study of site-directed mutagenesis of a reporter construct and chromatin immunoprecipitation revealed the importance of an E box Myc-binding motif located at position −103 to −98 from the transcription start sites, as well as an in vivo interaction between c-Myc and N-Myc and the proximal *ICAD* promoter. Furthermore, we demonstrated the functional importance of Myc proteins with regard to transcriptional regulation of the ICAD gene from studies examining ectopic expression of c-Myc and N-Myc, as well as with RNAi technology. We showed that expression levels of ICAD and Myc correlate in some tumors.

c-Myc and N-Myc are transcription factors of the bHLH LZ family that bind to the E box sequence within promoters to control proliferation, cell differentiation, and apoptosis [25, 31, 32]. *c-myc* and *N-myc* genes are deregulated in a number of human cancers and influence proliferation and growth. A link between Myc and cancer is well established both in vivo and in vitro, and onco-genic activation of Myc has been observed to promote the development of a number of clinically significant cancers [25, 33]. However, the molecular and cellular

mechanisms of Myc-mediated transformation are not fully understood. Although a variety of Myc target genes were identified and recruitment of Myc to the target promoters such as prothymosin and telomerase were shown [34], there has been no direct evidence on involvement of Myc in regulation of ICAD expression. It is known that c-Myc activation usually occurs during the later stages of carcinoma in humans. Conversely, in premalignant cells, c-Myc is a robust stimulator of apoptosis and programmed cell death [32]. One area of investigation into cancer cell death mechanisms centers on the mechanism by which c-Myc stimulates or suppresses apoptosis. For instance, Myc has been reported to potentiate apoptosis through both p53-dependent and -independent mechanisms [35, 36]. Myc controls the balance between pro- and anti-apoptotic factors at the level of the mitochondria, thereby regulating cytochrome C release and activation of downstream caspases [37, 38]. Involvement of Myc in up-regulation of ICAD expression as demonstrated in this study might present a novel mechanism of Myc-dependent inhibition of apoptosis. It is possible that elevated levels of ICAD in cells inhibit activation of endonuclear activity, thereby increasing the threshold for apoptosis signaling.

Kawane et al. have reported on the structure and analyzed the promoter of a murine *ICAD* gene, by which they demonstrated that a 118-bp flanking region of the *ICAD* gene is required for its transcription [16]. The mouse sequence shares approximately 82% homology with a corresponding upstream region of the human *ICAD* gene. The mouse *ICAD* promoter has a number of potential binding sites for transcription factors, such as Ikaros, c-Rel, Myc, and Gfi-1 [16]. Conservation of the Myc-binding motif among human and murine promoters suggests a functional significance of Myc in transcriptional regulation of *ICAD* expression.

In conclusion, this is the first report to identify a functional promoter of the human *ICAD* gene, and to demonstrate that Myc proteins are able to positively regulate ICAD gene expression. Extensive apoptosis research to date has shown that tumor aggression depends on various defects in apoptosis signaling [39]. Further investigation into the molecular events linking Myc expression with *ICAD* gene regulation may provide insight into Myc's role in cell proliferation, transformation and apoptosis.

References

1. Raff MC (1992) Social controls on cell survival and cell death. Nature 356:397–400. doi:10.1038/356397a0

2. Liu X, Zou H, Slaughter C, Wang X (1997) DFF, a heterodimeric protein that functions downstream of caspase-3 to trigger DNA fragmentation during apoptosis. Cell 89:175–184. doi:10.1016/S0092-8674(00)80197-X

3. Enari M, Sakahira H, Yokoyama H et al (1998) A caspase-activated DNase that degrades DNA during apoptosis, and its inhibitor ICAD. Nature 391:43–50. doi:10.1038/34112

4. Sabol SL, Li R, Lee TY, Abdul-Khalek R (1998) Inhibition of apoptosis-associated DNA fragmentation activity in nonapoptotic cells: the role of DNA fragmentation factor-45 (DFF45/ICAD). Biochem Biophys Res Commun 253:151–158. doi:10.1006/bbrc.1998.9770

5. Sakahira H, Enari M, Nagata S (1998) Cleavage of CAD inhibitor in CAD activation and DNA degradation during apoptosis. Nature 391:96–99. doi:10.1038/34214

6. Samejima K, Earnshaw WC (1998) ICAD/DFF regulator of apoptotic nuclease is nuclear. Exp Cell Res 243:453–459. doi:10.1006/excr.1998.4212

7. Nagata S (2000) Apoptotic DNA fragmentation. Exp Cell Res 256:12–18. doi:10.1006/excr.2000.4834

8. Nagata S, Nagase H, Kawane K et al (2003) Degradation of chromosomal DNA during apoptosis. Cell Death Differ 10:108–116. doi:10.1038/sj.cdd.4401161

9. Mukae N, Enari M, Sakahira H et al (1998) Molecular cloning and characterization of human caspase-activated DNase. Proc Natl Acad Sci USA 95:9123–9128. doi:10.1073/pnas.95.16.9123

10. Leek JP, Carr IM, Bell SM, Markham AF, Lench NJ (1997) Assignment of the DNA fragmentation factor gene (DFFA) to human chromosome bands 1p36.3->p36.2 by in situ hybridization. Cytogenet Cell Genet 79:212–213

11. Charrier L, Jarry A, Toquet C et al (2002) Growth phase-dependent expression of ICAD-L/DFF45 modulates the pattern of apoptosis in human colonic cancer cells. Cancer Res 62:2169–2174

12. Abel F, Sjoberg RM, Ejeskar K, Krona C, Martinsson T (2002) Analyses of apoptotic regulators CASP9 and DFFA at 1P36.2, reveal rare allele variants in human neuroblastoma tumours. Br J Cancer 86:596–604. doi:10.1038/sj.bjc.6600111

13. Konishi S, Ishiguro H, Shibata Y et al (2002) Decreased expression of DFF45/ICAD is correlated with a poor prognosis in patients with esophageal carcinoma. Cancer 95:2473–2478. doi:10.1002/cncr.10987

14. Brustmann H (2006) DNA fragmentation factor (DFF45): expression and prognostic value in serous ovarian cancer. Pathol Res Pract 202:713–720. doi:10.1016/j.prp.2006.06.003

15. Sacco R, Tsutsumi T, Suzuki R et al (2003) Antiapoptotic regulation by hepatitis C virus core protein through up-regulation of inhibitor of caspase-activated DNase. Virology 317:24–35. doi:10.1016/j.virol.2003.08.028

16. Kawane K, Fukuyama H, Adachi M et al (1999) Structure and promoter analysis of murine CAD and ICAD genes. Cell Death Differ 6:745–752. doi:10.1038/sj.cdd.4400547

17. Masaki T, Matsuura T, Ohkawa K et al (2006) All-trans retinoic acid down-regulates human albumin gene expression through the induction of C/EBPbeta-LIP. Biochem J 397:345–353. doi:10.1042/BJ20051863

18. Suzuki Y, Yamashita R, Sugano S, Nakai K (2004) DBTSS: DataBase of Transcriptional Start Sites: progress report 2004. Nucleic Acids Res 32:D78–D81. doi:10.1093/nar/gkh076

19. Wingender E, Dietze P, Karas H, Knuppel R (1996) TRANSFAC: a database on transcription factors and their DNA binding sites. Nucleic Acids Res 24:238–241. doi:10.1093/nar/24.1.238

20. Bello-Fernandez C, Packham G, Cleveland JL (1993) The ornithine decarboxylase gene is a transcriptional target of c-Myc. Proc Natl Acad Sci USA 90:7804–7808. doi:10.1073/pnas.90.16.7804

21. Meier JL, Luo X, Sawadogo M, Straus SE (1994) The cellular transcription factor USF cooperates with varicella-zoster virus immediate-early protein 62 to symmetrically activate a bidirectional viral promoter. Mol Cell Biol 14:6896–6906

22. Kiermaier A, Gawn JM, Desbarats L et al (1999) DNA binding of USF is required for specific E-box dependent gene activation in vivo. Oncogene 18:7200–7211. doi:10.1038/sj.onc.1203166

23. Luscher B, Larsson LG (1999) The basic region/helix-loop-helix/leucine zipper domain of Myc proto-oncoproteins: function and regulation. Oncogene 18:2955–2966. doi:10.1038/sj.onc.1202750

24. Grandori C, Cowley SM, James LP, Eisenman RN (2000) The Myc/Max/Mad network and the transcriptional control of cell behavior. Annu Rev Cell Dev Biol 16:653–699. doi:10.1146/annurev.cellbio.16.1.653

25. Adhikary S, Eilers M (2005) Transcriptional regulation and transformation by Myc proteins. Nat Rev Mol Cell Biol 6:635–645. doi:10.1038/nrm1703

26. Wagner AJ, Le Beau MM, Diaz M, OHay N (1992) Expression, regulation, and chromosomal localization of the Max gene. Proc Natl Acad Sci USA 89:3111–3115. doi:10.1073/pnas.89.7.3111

27. Skouteris GG, Schroder CH (1996) c-Myc and Max interactions in quiescent and mitogen-stimulated primary hepatocytes. Exp Cell Res 225:237–244. doi:10.1006/excr.1996.0173

28. Kato H, Okamura K, Kurosawa Y et al (1989) Characterization of DNA rearrangements of N-Myc gene amplification in three neuroblastoma cell lines by pulsed-field gel electrophoresis. FEBS Lett 250:529–535. doi:10.1016/0014-5793(89)80790-2

29. Masuoka J, Shiraishi T, Ichinose M, Mineta T, Tabuchi K (2001) Expression of ICAD-l and ICAD-S in human brain tumor and its cleavage upon activation of apoptosis by anti-Fas antibody. Jpn J Cancer Res 92:806–812

30. Yang HW, Chen YZ, Piao HY et al (2001) DNA fragmentation factor 45 (DFF45) gene at 1p36.2 is homozygously deleted and encodes variant transcripts in neuroblastoma cell line. Neoplasia 3:165–169. doi:10.1038/sj.neo.7900141

31. Secombe J, Pierce SB, Eisenman RN (2004) Myc: a weapon of mass destruction. Cell 117:153–156. doi:10.1016/S0092-8674(04)00336-8

32. Meyer N, Kim SS, Penn LZ (2006) The Oscar-worthy role of Myc in apoptosis. Semin Cancer Biol 16:275–287. doi:10.1016/j.semcancer.2006.07.011

33. Donaldson TD, Duronio RJ (2004) Cancer cell biology: Myc wins the competition. Curr Biol 14:R425–R427

34. Mac SM, D'Cunha CA, Farnham PJ (2000) Direct recruitment of N-Myc to target gene promoters. Mol Carcinog 29:76–86

35. Sakamuro D, Eviner V, Elliott KJ et al (1995) c-Myc induces apoptosis in epithelial cells by both p53-dependent and p53-independent mechanisms. Oncogene 11:2411–2418

36. Nilsson JA, Cleveland JL (2003) Myc pathways provoking cell suicide and cancer. Oncogene 22:9007–9021
37. Juin P, Hueber AO, Littlewood T, Evan G (1999) c-Myc-induced sensitization to apoptosis is mediated through cytochrome c release. Genes Dev 13:1367–1381
38. Hotti A, Jarvinen K, Siivola P, Holtta E (2000) Caspases and mitochondria in c-Myc-induced apoptosis: identification of ATM as a new target of caspases. Oncogene 19:2354–2362
39. Hanahan D, Weinberg RA (2000) The hallmarks of cancer. Cell 100:57–70

Arsenic Trioxide Inhibits Hepatitis C Virus RNA Replication through Modulation of the Glutathione Redox System and Oxidative Stress[∇]

Misao Kuroki,[1] Yasuo Ariumi,[1] Masanori Ikeda,[1] Hiromichi Dansako,[1]
Takaji Wakita,[2] and Nobuyuki Kato[1*]

*Department of Tumor Virology, Okayama University Graduate School of Medicine, Dentistry, and Pharmaceutical Sciences, 2-5-1,
Shikata-cho, Okayama 700-8558, Japan,[1] and Department of Virology II, National Institute of Infectious Diseases,
1-23-1 Toyama, Shinjuku-ku, Tokyo 162-8640, Japan[2]*

Arsenic trioxide (ATO), a therapeutic reagent used for the treatment of acute promyelocytic leukemia, has recently been reported to increase human immunodeficiency virus type 1 infectivity. However, in this study, we have demonstrated that replication of genome-length hepatitis C virus (HCV) RNA (O strain of genotype 1b) was notably inhibited by ATO at submicromolar concentrations without cell toxicity. RNA replication of HCV-JFH1 (genotype 2a) and the release of core protein into the culture supernatants were also inhibited by ATO after the HCV infection. To clarify the mechanism of the anti-HCV activity of ATO, we examined whether or not PML is associated with this anti-HCV activity, since PML is known to be a target of ATO. Interestingly, we observed the cytoplasmic translocation of PML after treatment with ATO. However, ATO still inhibited the HCV RNA replication even in the PML knockdown cells, suggesting that PML is dispensable for the anti-HCV activity of ATO. In contrast, we found that N-acetyl-cysteine, an antioxidant and glutathione precursor, completely and partially eliminated the anti-HCV activity of ATO after 24 h and 72 h of treatment, respectively. In this context, it is worth noting that we found an elevation of intracellular superoxide anion radical, but not hydrogen peroxide, and the depletion of intracellular glutathione in the ATO-treated cells. Taken together, these findings suggest that ATO inhibits the HCV RNA replication through modulation of the glutathione redox system and oxidative stress.

Hepatitis C virus (HCV) is the causative agent of chronic hepatitis, which progresses to liver cirrhosis and hepatocellular carcinoma. HCV is an enveloped virus with a positive single-stranded 9.6-kb RNA genome, which encodes a large polyprotein precursor of approximately 3,000 amino acid residues. This polyprotein is cleaved by a combination of the host and viral proteases into at least 10 proteins in the following order: core, envelope 1 (E1), E2, p7, nonstructural 2 (NS2), NS3, NS4A, NS4B, NS5A, and NS5B (30).

Alpha interferon has been used as an effective anti-HCV reagent in clinical therapy for patients with chronic hepatitis C. The current combination treatment with pegylated alpha interferon and ribavirin, a nucleoside analogue, has been shown to improve the sustained virological response rate to more than 50% (15). However, the adverse effects of the combination therapy and the limited efficacy against genotype 1b warrant the development of new anti-HCV reagents.

Arsenic trioxide (ATO) (As_2O_3, arsenite) has been used as a therapeutic reagent in acute promyelocytic leukemia, which bears an oncogenic PML-retinoic acid receptor alpha fusion protein resulting from chromosomal translocation (51, 52, 68, 70). The ATO treatment induces complete remission through degradation of the aberrant PML-retinoic acid receptor α (70). The PML tumor suppressor protein is required for formation

of the PML nuclear body (PML-NB), also known as nuclear dot 10 or the PML oncogenic domain, which is often disrupted by infection with DNA viruses, such as herpes simplex virus type 1, human cytomegalovirus, and Epstein-Barr virus (17). The treatment with ATO results in degradation of the PML protein and disruption of the PML-NB (70). Therefore, ATO has been become a useful probe for investigating the functions of the PML-NB, including cell growth, apoptosis, stress response, and viral infection. Indeed, ATO has been shown to increase retroviral infectivity, such as human immunodeficiency virus type 1 (HIV-1) and murine leukemia virus infectivity, but the mechanisms of this change are not well understood (5, 6, 32, 44, 47, 50, 57). In contrast, ATO was recently reported to inhibit the replication of HCV subgenomic replicon RNA (24). However, it also remains unclear how ATO inhibits the HCV RNA replication. In this study, using genome-length HCV RNA replication systems, we investigated the molecular mechanism(s) of the anti-HCV activity of ATO, and we provide evidence that ATO inhibits HCV RNA replication through modulation of the glutathione redox system and oxidative stress.

MATERIALS AND METHODS

Reagents. ATO, N-acetyl-cysteine (NAC), ascorbic acid (vitamin C), and L-buthionine sulfoximine (BSO) were purchased from Sigma (St. Louis, MO). Arsenic pentoxide (APO) (As_2O_5, arsenate) was purchased from Wako (Osaka, Japan). Both ATO and APO were dissolved in 1 N NaOH at 0.1 M as a stock solution. An inducible nitric oxide synthase (iNOS) inhibitor, 1400W, was purchased from Calbiochem (Merck Biosciences, Darmstadt, Germany).

Cell culture. 293FT cells were cultured in Dulbecco's modified Eagle's medium (Invitrogen, Carlsbad, CA, USA) supplemented with 10% fetal bovine serum. The following four HuH-7-derived cell lines or their parental HuH-7 cells

* Corresponding author. Mailing address: Department of Tumor Virology, Okayama University Graduate School of Medicine, Dentistry, and Pharmaceutical Sciences, 2-5-1, Shikata-cho, Okayama 700-8558, Japan. Phone: 81 86 235 7385. Fax: 81 86 235 7392. E-mail: nkato@md.okayama-u.ac.jp.

were cultured in Dulbecco's modified Eagle's medium with 10% fetal bovine serum as described previously (25); O cells, harboring a replicative genome-length HCV-O RNA (O strain of genotype 1b) (25); OR6 cells, harboring the genome-length HCV-O RNA with luciferase as a reporter (25); sO cells, harboring the subgenomic replicon RNA of HCV-O (31); and RSc cured cells, which cell culture-generated HCV-JFH1 (JFH1 strain of genotype 2a) (58) could infect and effectively replicate in (2, 3). The O, OR6, and sO cells were maintained in the presence of G418 (300 μg/ml Geneticin; Invitrogen).

RNA interference. Oligonucleotides with the following sense and antisense sequences were used for the cloning of short hairpin RNA (shRNA)-encoding sequences targeted to PML (56) in a lentiviral vector: 5'-GATCCCCAGATGC AGCTGTATCCAAGTTCAAGAGACTTGGATACAGCTGCATCTTTTTTG GAAA-3' (sense) and 5'-AGCTTTTCCAAAAAAGATGCAGCTGTATCCAA GTCTCTTGAACTTGGATACAGCTGCATCTGGG-3' (antisense). These oligonucleotides were annealed and subcloned into the BglII-HindIII site, downstream from an RNA polymerase III promoter of pSUPER (8), to generate pSUPER-PMLi. To construct pLV-PMLi, the BamHI-SalI fragments of pSUPER-PMLi were subcloned into the BamHI-SalI site of pRDI292, an HIV-1-derived self-inactivating lentiviral vector containing a puromycin resistance marker allowing for the selection of transduced cells (7). pLV-Chk2i was described previously (3).

Lentiviral vector production. The vesicular stomatitis virus (VSV) G-pseudotyped HIV-1-based vector system has been described previously (42). The lentiviral vector particles were produced by transient transfection of the second-generation packaging construct pCMV-ΔR8.91 (1, 71) and the VSV G envelope-expressing plasmid pMDG2 as well as pRDI292 into 293FT cells with FuGene6 (Roche Diagnostics, Mannheim, Germany).

HCV infection experiments. The supernatants was collected from cell culture-generated HCV-JFH1 (58)-infected RSc cells (2, 3) at 5 days postinfection and stored at −80°C after filtering through a 0.45-μm filter (Kurabo, Osaka, Japan) until use. For infection experiments with HCV-JFH1 virus, RSc cells (1 × 10^5 cells/well) were plated onto six-well plates and cultured for 24 h. We then infected the cells with 50 μl (equivalent to a multiplicity of infection of 0.05 to 0.1) of inoculum. The culture supernatants were collected at 97 h postinfection, and the levels of the core protein were determined by enzyme-linked immunosorbent assay (Mitsubishi Kagaku Bio-Clinical Laboratories, Tokyo, Japan). Total RNA was isolated from the infected cellular lysates using an RNeasy minikit (Qiagen, Hilden, Germany) for quantitative reverse transcription-PCR (RT-PCR) analysis of intracellular HCV RNA. The level of intracellular HCV RNA in the RSc cells was >10^8 copies/μg total RNA at 4 days postinfection.

Quantitative RT-PCR Analysis. The quantitative RT-PCR analysis for HCV RNA was performed by real-time LightCycler PCR (Roche) as described previously (25). We used the following forward and reverse primer sets for the real-time LightCycler PCR: PML, 5'-GAGGAGTTCCAGTTTCTGCG-3' (forward), 5'-GCGCCTGGCAGATGGGGCAC-3' (reverse); β-actin, 5'-TGACGG GGTCACCCACACTG-3' (forward), 5'-AAGCTGTAGCCGCGCTCGGT-3' (reverse); HCV-O, 5'-AGAGCCATAGTGGTCTGCGG-3' (forward), 5'-CTT TCGCGACCCAACACTAC-3' (reverse); and HCV-JFH1, 5'-5'-AGAGCCAT AGTGGTCTGCGG-3' (forward), 5'-CTTTCGCAACCCAACGCTAC-3' (reverse).

Western blot analysis. Cells were lysed in buffer containing 50 mM Tris-HCl (pH 8.0), 150 mM NaCl, 4 mM EDTA, 1% Nonidet P-40, 0.1% sodium dodecyl sulfate, 1 mM dithiothreitol, and 1 mM phenylmethylsulfonyl fluoride. Supernatants from these lysates were subjected to sodium dodecyl sulfate-polyacrylamide gel electrophoresis, followed by immunoblot analysis using anti-PML (A301-168A-1; Bethyl Laboratories, Montgomery, TX), anti-Chk2 (DCS-273; Medical & Biological Laboratories, MBL, Nagoya, Japan), anti-HCV core (CP-9 and CP-11; Institute of Immunology, Tokyo, Japan), anti-HCV NS5A (no. 8926; a generous gift from A Takamizawa, The Research Foundation for Microbial Diseases of Osaka University, Japan), anti-signal transducer and activator of transcription 3 (anti-STAT3) (BD Bioscience, San Jose, CA), anti-phospho-STAT3 (Tyr705) (Cell Signaling Technology, Danvers, MA) anti-poly(ADP-ribose) polymerase 1 (anti-PARP-1) (C-2-10; Calbiochem), or anti-β-actin antibody (Sigma).

MTT assay. HuH-7 or O cells (5 × 10^3 cells/well) were plated onto 96-well plates and cultured for 24 h. The cells were treated with ATO, APO, or NaOH for 24, 48, or 72 h and then subjected to the colorimetric 3-(4,5-dimethylthiazol-2-yl)-2,5-diphenyltetrazolium bromide (MTT) assay according to the manufacturer's instructions (cell proliferation kit I; Roche). The absorbance was read using a microplate reader (model 2550; Bio-Rad Laboratories, Hercules, CA) at 550 nm with a reference wavelength of 690 nm.

RL assay. OR6 cells (1.5 × 10^4 cells/well) were plated onto 24-well plates and cultured for 24 h. The cells were treated with each reagent for 72 h and then

subjected to the *Renilla* luciferase (RL) assay according to the manufacturer's instructions (Promega, Madison, WI). A Lumat LB9507 luminometer (Berthold, Bad Wildbad, Germany) was used to detect RL activity.

FL assay. Plasmids were transfected into O cells (2 × 10^4 cells/well in 24-well plates) using FuGene6 and cultured for 24 h. The cells were treated with or without 1 μM ATO for 24 h, and then firefly luciferase (FL) assays were performed according to the manufacturer's instructions (Promega).

Immunofluorescence and confocal microscopic analysis. Cells were fixed in 3.6% formaldehyde in phosphate-buffered saline (PBS), permeabilized in 0.1% NP-40 in PBS at room temperature, and incubated with anti-PML antibody (PM001; MBL) at a 1:300 dilution in PBS containing 3% bovine serum albumin at 37°C for 30 min. They were then stained with fluorescein isothiocyanate-conjugated anti-rabbit antibody (Jackson ImmunoResearch, West Grove, PA) at a 1:300 dilution in PBS containing bovine serum albumin at 37°C for 30 min, followed by staining with 4',6-diamidino-2-phenylindole (DAPI) at room temperature for 15 min. Following extensive washing in PBS, the cells were mounted on slides using a mounting medium of 90% glycerin–10% PBS with 0.01% p-phenylenediamine added to reduce fading. Samples were viewed under a confocal laser-scanning microscope (LSM510; Zeiss, Jena, Germany).

Measurement of intracellular O$_2^-$ and H$_2$O$_2$ production. The intracellular superoxide anion radical (O$_2^-$) levels were measured with an oxidation-sensitive fluorescent probe, dihydroethidium (DHE) (Invitrogen Molecular Probes), that is highly selective for detection of O$_2^-$ among reactive oxygen species (ROS). DHE is cell permeative and reacts with O$_2^-$ to form ethidium, which in turn intercalates in DNA, thereby exhibiting a red fluorescence. The intracellular hydrogen peroxide (H$_2$O$_2$) levels were measured with another oxidation-sensitive fluorescent probe dye, 6-carboxy-2',7'-dichlorodihydrofluorescein diacetate (carboxy-H$_2$DCFDA) (Invitrogen Molecular Probes). Carboxy-H$_2$DCFDA was intracellularly deacetylated with esterase and further oxidized with peroxidase to the fluorescent 2',7'-dichlorodihydrofluorescein (DCF). The ATO- or BSO-treated O cells were washed with PBS and incubated with 5 μM DHE and 20 μM carboxy-H$_2$DCFDA in PBS at 37°C for 30 min. Cells were then washed twice with PBS. The DHE or DCF fluorescence intensity was measured using a FACS-Calibur flow cytometer. For each sample, 10,000 events were collected. The O$_2^-$ or H$_2$O$_2$ levels are indicated as mean fluorescence intensities, which were determined with the CellQuest software (BD Bioscience).

Detection of intracellular glutathione. Intracellular glutathione levels were analyzed using CellTracker Green (5-chloromethylfluorescein diacetate [CMFDA]; Molecular Probes, Invitrogen). CMFDA is a membrane-permeative dye used to determine intracellular glutathione levels. Cytoplasmic esterase converts the nonfluorescent CMFDA to the fluorescent 5-chloromethylfluorescein (CMF), which can then react with glutathione. The excitation peak is at 492 nm, and the fluorescence emission peak is at 517 nm. O cells treated with 1 μM ATO for 72 h were washed with PBS and incubated with 5 μM CMFDA at 37°C for 30 min. The CMF fluorescence intensity was measured using a FACSCalibur flow cytometer. For each sample, 10,000 events were collected. The glutathione levels are given as the relative mean fluorescence intensities, which were determined with CellQuest software.

RESULTS

ATO inhibits HCV RNA replication. First, we quantitatively examined the effect of ATO on the HCV RNA replication in HuH-7-derived O cells harboring a replicative genome-length HCV-O RNA (25). We found that submicromolar concentrations of ATO markedly inhibited genome-length HCV-O RNA replication in the O cells at 72 h after administration (Fig. 1A). The 50% effective concentration (EC$_{50}$) of ATO required for inhibition of genome-length HCV-O RNA replication is 0.19 μM (Fig. 1A). Consistent with this finding, the expression levels of the HCV core and NS5A proteins were also significantly decreased in the cell lysates of O cells treated with ATO for 72 h (Fig. 1B). In addition, ATO markedly inhibited the replication of the subgenomic replicon RNA (31), with an EC$_{50}$ of 0.48 μM at 72 h after the treatment (Fig. 1C). We next examined the effect of ATO on HCV reproduction by HCV-JFH1 infection (58). The results revealed that ATO significantly inhibited the intracellular RNA replication of HCV-
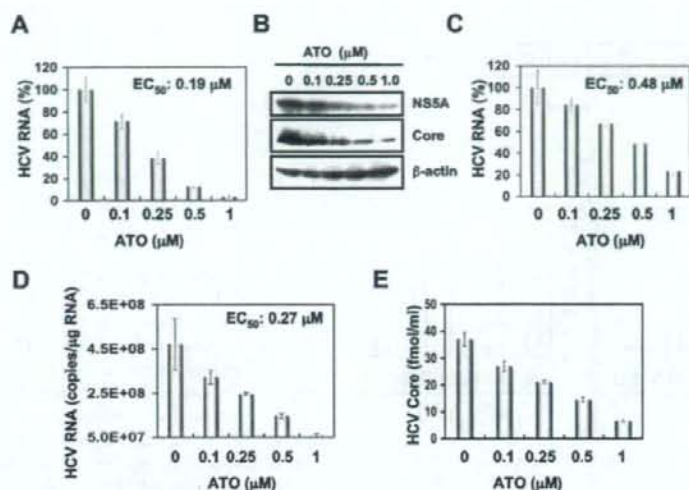
FIG. 1. Inhibition of HCV RNA replication by ATO. (A) The level of genome-length HCV RNA in O cells after the treatment with ATO was monitored by real-time LightCycler PCR. Experiments were done in triplicate and, bars represent the mean percentage of HCV RNA. Error bars indicate standard deviations. (B) HCV core and NS5A protein expression levels in O cells after treatment with ATO. The results of Western blot analysis of cellular lysates with anti-HCV core, anti-HCV NS5A, or anti-β-actin antibody in O cells at 72 h after treatment with ATO at the indicated concentration are shown. (C) The level of subgenomic replicon RNA was monitored by real-time LightCycler PCR. Results from three independent experiments conducted as described for panel A are shown. (D) The level of intracellular genome-length HCV-JFH1 RNA was monitored by real-time LightCycler PCR. RSc cells were pretreated with the indicated concentration of ATO for 13 h, followed by inoculation of the HCV-JFH1 virus, and then the infected cells were further incubated with ATO for 97 h. Results from three independent experiments conducted as described for panel A are shown. (E) The levels of the core protein in the culture supernatants treated as described for panel D were determined by enzyme-linked immunosorbent assay. Experiments were done in triplicate, and bars represent the mean core protein levels.

JFH1, with an EC_{50} of 0.27 μM, as well as the release of core protein into the culture supernatants in HuH-7-derived RSc cells at 97 h after inoculation of the HCV-JFH1 virus (Fig. 1D and E). Thus, we have demonstrated for the first time that ATO can inhibit the reproduction of HCV and particularly HCV RNA replication.

Effect of APO on HCV replication. Arsenic is known to exist in two oxidation states, As(III) in ATO and As(V) in APO. As ATO in the lower valence state has been reported to be more toxic than APO (48), we compared their anti-HCV activities using an OR6 assay system, which was recently developed as a luciferase reporter assay system for monitoring genome-length HCV RNA replication in HuH-7-derived OR6 cells (Fig. 2A) (25). The results showed that APO could not strongly suppress HCV replication at submicromolar concentrations, while ATO strongly inhibited it, with an EC_{50} of 0.33 μM (Fig. 2B and C), indicating that ATO has unique anti-HCV activity. In this context, it is relevant that the expression level of HCV core protein was also remarkably decreased in the cell lysates of O cells treated with ATO, but not those treated with APO, for 72 h (Fig. 2D). Thus, APO seems to be a useful negative probe to clarify the mechanism of the anti-HCV activity of ATO.

ATO does not affect cell growth at submicromolar concentrations. ATO has been reported to induce apoptosis (11, 14, 20, 21, 26–28, 33, 48, 66). Therefore, such an ATO-induced apoptosis may be involved in the anti-HCV activity. To test this possibility, we examined the effect of ATO or APO at various concentrations on cell proliferation by colorimetric MTT assay. In this context, we demonstrated that ATO did not affect

the cell proliferation of O cells or the parental HCV-negative HuH-7 cells at submicromolar concentrations (Fig. 3A and E). In contrast, 4 or 8 μM ATO significantly inhibited cell proliferation (Fig. 3B and F). Similarly, APO did not affect the cell proliferation at less than 2 μM (Fig. 3C and D). Consistent with the above results, ATO-treated O cells exhibited normal growth rates and cell viabilities, at least at 1 μM for 72 h (Fig. 3G). Furthermore, we did not observe the cleavage of PARP-1, which is known to be an important substrate for activated caspase 3, in O cells treated with 1 μM ATO at least until 72 h (Fig. 3H), indicating that 1 μM ATO did not induce apoptosis in O cells. Thus, we concluded that the anti-HCV activity was independent of ATO-induced apoptosis or cell toxicity, at least at submicromolar concentrations.

PML and Chk2 are dispensable for the anti-HCV activity of ATO. Since PML is known to be a target of ATO (70), we first examined the subcellular localization of PML in O cells treated with either 1 μM ATO or 1 μM APO for 72 h by means of an anti-PML antibody (PM001; MBL) that can recognize most of the PML splicing variants and is useful for immunofluorescence analysis. The results showed that PML was localized predominantly in punctate nuclear speckles termed PML-NBs in control O cells (Fig. 4A). Interestingly, we noticed that some nuclear PML, but not all, disappeared and was translocated into discrete cytoplasmic bodies in the O cells treated with 1 μM ATO (Fig. 4A). We also observed cytoplasmic translocation of PML in the O cells treated with 1 μM APO for 72 h (Fig. 4A). Furthermore, we observed a similar cytoplasmic translocation of PML in the HCV-negative 293FT or HeLa
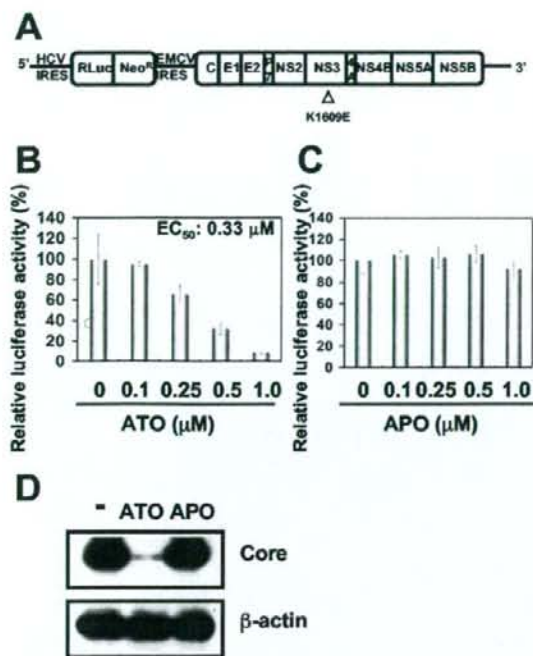
FIG. 2. Effect of APO on HCV replication. (A) Schematic representation of genome-length HCV RNA encoding the RL gene as a reporter (ORN/C-5B/KE RNA) replicated in OR6 cells. The RL is expressed as a fusion protein with neomycin phosphotransferase (Neo^R). The position of an adaptive mutation, K1609E in NS3, is indicated by an open triangle. (B) Effect of ATO on genome-length HCV RNA replication. At 72 h after treatment of OR6 cells with ATO at the indicated concentrations, the replication level of HCV RNA was monitored by the RL assay. The relative RL activity is shown. The results shown are means from three independent experiments. Error bars indicate standard deviations. (C) Effect of APO on genome-length HCV RNA replication. At 72 h after treatment of OR6 cells with APO at the indicated concentrations, the replication level of HCV RNA was monitored by the RL assay as described for panel B. (D) HCV core protein expression level in O cells after treatment with either ATO or APO. The results of Western blot analysis of cellular lysates with anti-HCV core or anti-β-actin antibody in O cells at 72 h after treatment with either 1 μM ATO or 1 μM APO are shown.

cells after the treatment with ATO (data not shown). Thus, we concluded that the cytoplasmic translocation of PML after the treatment with ATO was not associated with anti-HCV activity. Next, Western blot analysis to compare PML expression in the lysates of O cells treated with 1 μM ATO or 1 μM APO for 72 h was performed using another anti-PML antibody, A301-168A-1 (a gift from Bethyl Laboratories), which can recognize the longest isoform, PML I, but not shorter PML isoforms such as PML VI and which has been proven useful for Western blot analysis. Consistent with the previous finding that ATO promotes PML degradation (70), the expression level of the PML I protein was lower in the ATO-treated O cells than in the APO-treated O cells (Fig. 4B), suggesting that PML degradation by ATO is associated with anti-HCV activity. To further examine whether PML is directly involved in the anti-HCV

activity of ATO, we used lentiviral vector-mediated RNA interference to stably knock down PML in the O cells. To express an shRNA targeted to all PML isoforms (56), we used the VSV G-pseudotyped HIV-1-based vector system (1, 42, 71). We used the puromycin-resistant pooled cells at 10 days after the lentiviral transduction in this experiment. Immunofluorescence and Western blot analysis demonstrated a very effective knockdown of PML in the O cells (Fig. 4C and D). We quantitatively examined the level of HCV RNA in the PML knockdown O cells treated with or without either 1 μM ATO (Fig. 4E) or 1 μM APO (Fig. 4F) for 72 h. The results showed that the replication level of genome-length HCV-O RNA in the untreated PML knockdown cells was similar to that in control cells (Fig. 4E), suggesting that PML is dispensable in HCV RNA replication. Importantly, ATO effectively inhibited the HCV RNA replication in both the PML knockdown cells and control cells compared with that of the APO-treated cells (Fig. 4E and F). Thus, we concluded that PML was dispensable for the anti-HCV activity of ATO. Since the Chk2 checkpoint kinase has recently been implicated in ATO-induced apoptosis and in association with PML (27, 63, 64, 66), we examined the anti-HCV activity in the ATO-treated Chk2 knockdown O cells (3). As we previously described, Western blot analysis demonstrated very effective knockdown of Chk2 in O cells (Fig. 4G). Accordingly, we examined the level of HCV RNA in Chk2 knockdown cells treated with or without either 1 μM ATO (Fig. 4H) or 1 μM APO (Fig. 4I) for 72 h. Consistent with our recent finding that Chk2 is required for HCV RNA replication, the replication of genome-length HCV RNA in the untreated Chk2 knockdown cells was remarkably suppressed (Fig. 4H). However, ATO strongly inhibited the HCV RNA replication in the Chk2 knockdown cells compared with that in the APO-treated Chk2 knockdown cells (Fig. 4H and I), suggesting that Chk2 is not implicated in the anti-HCV activity of ATO.

Effect of ATO on the stress-signaling pathways. To date, the focus has been on PML and PML-retinoic acid receptor α as major targets of ATO (70). On the other hand, arsenic has been reported to modulate other cell-signaling pathways, especially stress-responsive transcription factors, such as nuclear factor κB (NF-κB), activator protein 1 (AP-1), and STAT3 (12, 37, 38, 62). Therefore, we examined the involvement of several stress-responsive pathways in the anti-HCV activity of ATO by luciferase-based reporter assays or Western blot analysis using an antibody which specifically recognizes STAT3 phosphorylated at tyrosine 705. Although it has been reported that ATO inhibited the NF-κB signaling pathway through a direct interaction with IKKβ at a high concentration (more than 10 μM) (29), neither 1 μM ATO nor 1 μM APO affected the endogenous NF-κB transcriptional activity in the present study (Fig. 5A and B). Conversely, ATO at least slightly stimulated mitogen-activated protein kinase kinase kinase (MEKK)-mediated NF-κB activation (Fig. 5A and B). Since NF-κB activation has been shown to stimulate HCV replication (60), the NF-κB pathway would seem not to be essential for the anti-HCV activity of ATO. Next, regarding the AP-1 signaling pathway, both ATO and APO are known to activate c-Jun N-terminal kinase (JNK) (45). Importantly, there was no stimulation of JNK activity at a dose below 30 μM (45). In fact, 50 μM ATO but not 50 μM APO strongly stimulates AP-1 activity by in-
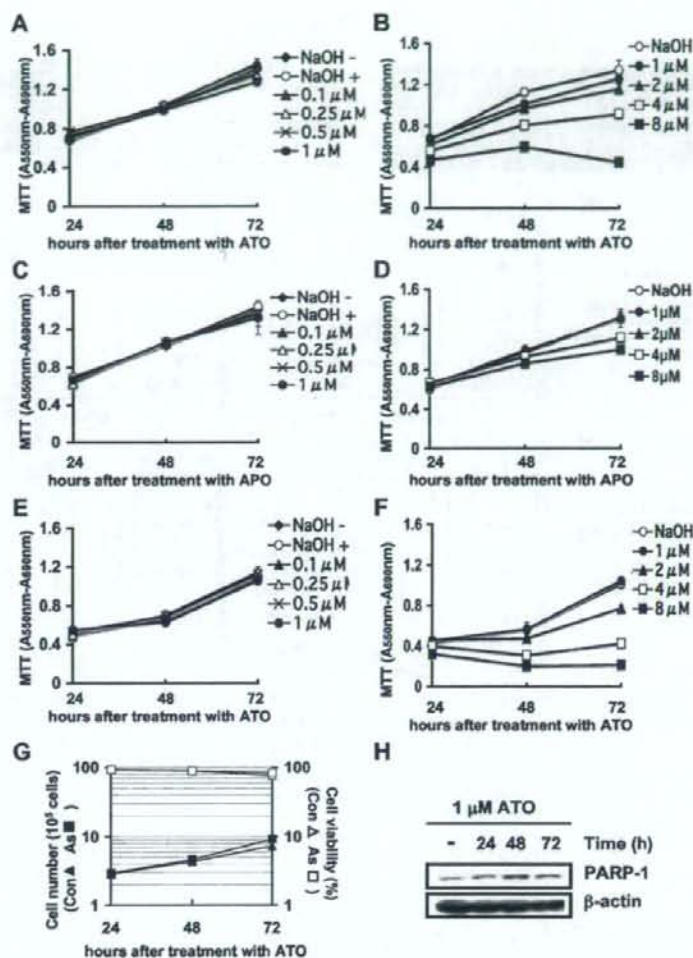
FIG. 3. Effect of ATO on cell growth and viability. (A and B) MTT assay of O cell lysates at the indicated times after treatment with ATO at various concentrations. NaOH (10 μM) was used as the solvent for ATO. The results shown are means from three independent experiments. Error bars indicate standard deviations. (C and D) MTT assay of O cell lysates at the indicated times after treatment with APO at various concentrations. (E and F) MTT assay of HuH-7 cell lysates at the indicated times after treatment with ATO at various concentrations. (G) Growth curve and viability of O cells after treatment with either 10 μM NaOH (Con) or 1 μM ATO (As). (H) Western blot analysis of cellular lysates with anti-PARP-1 or anti-β-actin antibody in O cells at the indicated times after treatment with 1 μM ATO.

hibiting a JNK phosphatase (10). Consistently, we found that both 1 μM ATO and 1 μM APO had a marginal effect on the AP-1 signaling pathway (Fig. 5C and D), suggesting that the AP-1 pathway is also not involved in the anti-HCV activity of ATO. Regarding the STAT3 signaling pathway, ATO has been reported to inhibit the phosphorylation of the STAT3 tyrosine at 705, leading to inactivation of the JAK-STAT signaling pathway (12, 62). In contrast, it has been reported that HCV constitutively phosphorylates and activates STAT3 (49, 59, 67). In this context, we observed constitutive tyrosine phosphorylation of STAT3 in untreated O cells (Fig. 5E). Furthermore, the marginal effect of 1 μM ATO on STAT3 phosphorylation

and interleukin-6-mediated STAT3 activation was also observed (Fig. 5E and F). Taken together, these results at least suggest that the NF-κB, AP-1, and STAT3 pathways may not be associated with the anti-HCV activity of ATO at submicromolar concentrations.

The anti-HCV activity of ATO is associated with the glutathione redox system and oxidative stress. Finally, we focused on the involvement of the glutathione redox system and oxidative stress in the anti-HCV activity of ATO. For this, we analyzed the HCV replication level after combination treatment with ATO and antioxidants such as NAC and vitamin C using the OR6 assay system. When OR6 cells were treated with
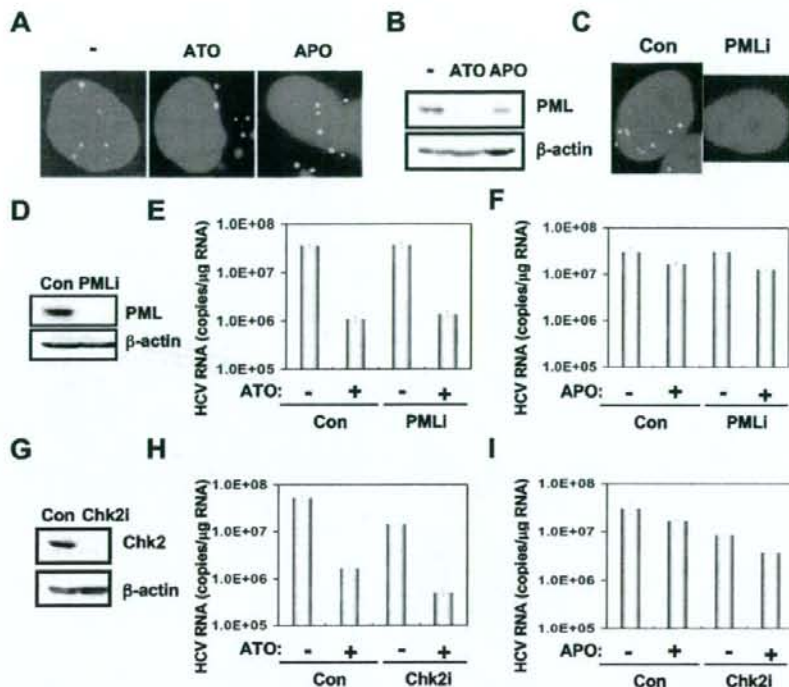
FIG. 4. PML and Chk2 are not required for the anti-HCV activity of ATO. (A) Subcellular localization of PML in O cells at 72 h after treatment with 10 μM NaOH (−), 1 μM ATO, or 1 μM APO. PML was detected by indirect immunofluorescence analysis with anti-PML antibody (PM001). DAPI staining of the nuclear DNA is also shown. (B) Induction of PML degradation by ATO but not by APO. The results of Western blot analysis of cellular lysates of O cells at 72 h after treatment with 10 μM NaOH (−), 1 μM ATO, or 1 μM APO with anti-PML (A301-168A-1) or anti-β-actin antibody are shown. (C) Stable knockdown of PML by shRNA-producing lentiviral vector in O cells. PML was detected by indirect immunofluorescence analysis with anti-PML antibody (PM001) in O cells expressing shRNA targeted to PML (PMLi) as well as in O cells transduced with a control lentiviral vector (Con). (D) Western blot analysis of cellular lysates with anti-PML (A301-168A-1) or anti-β-actin antibody in PML knockdown O cells (PMLi) as well as in control O cells (Con). (E and F) The level of genome-length HCV-O RNA was monitored by real-time LightCycler PCR in PML knockdown O cells (PMLi) as well as in control O cells (Con) after treatment with 10 μM NaOH (−), 1 μM ATO (+) (E), or 1 μM APO (+) (F) for 72 h. Results from three independent experiments conducted as described in the legend to Fig. 1A are shown. (G) Inhibition of Chk2 expression by shRNA-producing lentiviral vector. The results of Western blot analysis of cellular lysates with anti-Chk2 or anti-β-actin antibody in O cells expressing shRNA targeted to Chk2 (Chk2i) as well as in O cells transduced with a control lentiviral vector (Con) are shown. (H and I) The level of genome-length HCV-O RNA was monitored by real-time LightCycler PCR in Chk2 knockdown O cells (Chk2i) as well as in control O cells (Con) after treatment with 10 μM NaOH (−), 1 μM ATO (+) (H), or 1 μM APO (+) (I) for 72 h. Results from three independent experiments conducted as described in the legend to Fig. 1A are shown.

either 100 μM vitamin C or 10 mM NAC alone for 24 h or 72 h, the HCV replication was slightly enhanced (Fig. 6A and B), indicating that the antioxidant can activate HCV replication. Although the anti-HCV activity in the OR6 cells treated with 1 μM ATO and in combination with 100 μM vitamin C for 24 h was weakly reduced, 10 mM NAC completely and partially eliminated the anti-HCV activity of ATO after 24 h (Fig. 6A) and 72 h (Fig. 6B) of treatment, respectively, suggesting that oxidative stress and the glutathione redox system are associated with the anti-HCV activity of ATO. In contrast, the iNOS inhibitor 1400W did not suppress the HCV RNA replication or eliminate the anti-HCV activity of ATO, suggesting that NO is not involved in the anti-HCV activity of ATO (Fig. 6C). To further examine the involvement of oxidative stress in the anti-HCV activity of ATO, we examined ROS production in ATO-treated cells using two oxidative-sensitive fluorescent probes, DHE for detection of intracellular O_2^- and DCF for detection of intracellular H_2O_2. We found that 1 μM ATO could generate a significant level of intracellular O_2^- but not intracellular H_2O_2, while 2 μM BSO, an inhibitor of glutathione synthesis (14, 20, 33), could induce both O_2^- and H_2O_2 (Fig. 6D to H). Importantly, NAC diminished the ATO-dependent O_2^- induction (Fig. 6F). Since glutathione is a major antioxidant in cells and can clear away superoxide anion free radical, we also analyzed the changes of the intracellular glutathione level in ATO-treated O cells using CMF fluorescence, which can react with glutathione. As a result, we observed significant glutathione depletion in the cells treated with at least 1 μM ATO (Fig. 6I). To further confirm the involvement of glutathione in the anti-HCV activity of ATO, we examined the effect of cotreatment with ATO and BSO. When the OR6 cells were treated with 1 μM BSO alone, the HCV replication